



# Effect of size variation of fibre-shaped waste tyre rubber as fine aggregate on the ductility of self-compacting concrete

Akshay Anil Thakare<sup>1</sup> · Amardeep Singh<sup>2,3</sup> · Trilok Gupta<sup>4</sup> · Sandeep Chaudhary<sup>5,6</sup>

Received: 5 October 2021 / Accepted: 3 October 2022 / Published online: 15 October 2022  
© The Author(s), under exclusive licence to Springer-Verlag GmbH Germany, part of Springer Nature 2022

## Abstract

Abandoning shredded waste tyre rubber (WTR) in cement-based mixes facilitates safe waste tyre disposal and conserves the natural resources used in construction materials. The engineering properties of such environment-friendly materials needed to be evaluated for field applications. This study examined integrating WTR fibre on microstructural, static load, and ductility properties of self-compacting concrete (SCC). The WTR fibre of 0.60–1.18-, 1.18–2.36-, and 2.36–4.75-mm sizes was used as fine aggregate at 10%, 20%, and 30% replacement levels. Microstructural characterisation of hardened concrete specimens was done by scanning electron microscopy. The compressive strength and static modulus of elasticity tests were used to examine static load resistance, while drop weight and rebound impact tests were used to investigate impact load resistance. The water permeability test was performed as a measure of the durability of SCC with WTR fibre. Relationships have been studied between dynamic MOE and impact tests and rebound and drop weight impact testing. The Weibull two-parameter distribution was used to analyse the drop weight test statically. The results show that WTR fibre size variations efficiently lowered the concrete stiffness reducing the brittleness. Furthermore, incorporating WTR fibre improved the impact resistance of SCC.

**Keywords** Waste tyre rubber · Self-compacting concrete · Water permeability · Rebound impact · Drop weight impact · Weibull distribution

## Introduction

Along with the rapid infrastructural growth worldwide, the demand for the constituents of cementitious mixes is also increasing enormously. Fulfilling the demand for the constituents of cementitious mixes requires the extraction of natural resources such as mining river beds for sand, excavating mountain beds for acquiring rocks/boulders/coarse aggregates, and consuming limestones for cement manufacturing. The concrete mixes comprise nearly 60–80% of fine and coarse aggregates, which demands a high amount of natural fine/coarse aggregate (Yaragal et al. 2019). The natural river sand/crushed stones are conventionally used as fine aggregate for cementitious mixes. However, producing natural fine aggregates (NFA) leads to ecological threats due to the massive excavation of earth's surfaces, pollution during transportation and machine operations, and energy consumption (Gupta et al. 2016). Moreover, natural resources are limited and will be destroyed in the near future if not preserved carefully. Therefore, researchers explored viable alternate materials such as waste tyre rubber (WTR),

---

Responsible Editor: Philippe Garrigues

✉ Sandeep Chaudhary  
schaudhary@iiti.ac.in

<sup>1</sup> Department of Civil Engineering, Matoshri College of Engineering and Research Centre, Nasik 422105, India

<sup>2</sup> Department of Civil Engineering and Architecture, Changzhou Institute of Technology, Jiangsu, China

<sup>3</sup> Department of Structural Engineering, Tongji University, Shanghai 200092, China

<sup>4</sup> Department of Civil Engineering, College of Technology and Engineering, Maharana Pratap University of Agriculture & Technology, Udaipur 313001, India

<sup>5</sup> Department of Civil Engineering, Indian Institute of Technology Indore, Simrol, Indore 453552, India

<sup>6</sup> Center for Rural Development and Technology, Indian Institute of Technology Indore, Simrol, Indore 453552, India

kaolin tailings, offshore sand, sillimanite sand, processed lateritic sand, fine bone China ceramic, and waste granite to replace NFA fully/partially in cementitious mixes (Arulmoly et al. 2021, H. Gupta et al. 2021a, b, Jain et al. 2020, 2021, Siddique et al. 2019, Thakare et al. 2022a, Xu et al. 2018, Yaragal et al. 2019). Among the various alternate materials, researchers recognise WTR as fine aggregates for improving concrete's resilience and life-span (Li et al. 2004b).

Rubber wastes are one of the significant contributors to global solid waste. Worldwide, around 30 million tons of rubber tyres are disposed of every year due to the end-of-their life span (Recycling magazine 2020). The waste tyres are classified as non-biodegradable, and their disposal is an environmental concern (Girskas and Nagrockienė 2017; Rahat Dahmardeh et al. 2019; Thakare et al. 2020b). Conventional tyre disposal methods, such as dumping into open landfills/stockpiling in graveyards, and burning for fuel conversion, damage the natural ecosystem (Ghasemzadeh et al. 2021; Shen et al. 2013; Shu and Huang 2014; Sibeko et al. 2020). As a waste management technique, waste tyres are recycled to manufacture everyday products such as straps, footwear, and flooring pads, as well as industrial products such as cushioning sheets, mats, and new rubber tyres, all of which contribute to the recycling of 40% of waste tyres (Ba Thai et al. 2019). Even though waste tyres are recycled in industry and household products, significant numbers of waste tyres are left unattended for appropriate disposal.

For large-scale recycling, researchers have explored waste tyre applications in the construction industry as embankment backfilling material (Mohajerani et al. 2020), shock/impact-absorbing (the crash barrier), and water/soil retaining structures (Callinan and Cashman 2005; Mistry et al. 2021), seismic isolation systems (Tsang et al. 2007), and artificial reef construction (Chapman and Clynick 2006). Additionally, waste tyres are shredded into various sizes and shapes for usage as a constituent in cementitious mixes (Al-Mutairi et al. 2010; Da Silva et al. 2015; Fernández-Ruiz et al. 2018; Long et al. 2014; Reda Taha et al. 2008). The mechanical, pyrolysis or cryogenic processing of the waste tyres are needed for implementing WTR in cementitious mixes, which produce chipped, crumb, and powder form of WTR (Najim and Hall 2010; Pacheco-Torgal et al. 2012; Zamanzadeh et al. 2015).

Various researchers (Karimi et al. 2020; Nematzadeh et al. 2021; Nematzadeh and Mousavi 2021; Sabetifar et al. 2022) have explored the applications of crumbs of WTR as a replacement for NFA in cementitious mixes. In an analytical study, Karimi et al. (2020) found the effect of the volume ratio of steel fibre, tyre rubber content, diameter-to-thickness ( $D/t$ ) ratio of the steel tube, and exposure temperature, on the post-heating behaviour of concrete-filled steel tubular columns containing tyre rubber using finite element modelling in ABAQUS software. In a study, Nematzadeh et al. (2021)

used crumbs of WTR as NFA up to 10% replacement levels in glass fibre-reinforced polymer (GFRP) bar-reinforced high-strength concrete beams containing steel fibre to study the shear behaviour. They found the incorporation of crumbs of WTR decreased the shear capacity of the beam, while at the higher steel fibre content, the failure mode changed from shear to flexure. In another study, Nematzadeh and Mousavi (2021) investigated the post-fire flexural properties, i.e., flexure, stiffness, fracture energy, and toughness of one-layered, two-layered and three-layered functionally graded steel fibre-reinforced concrete at 23°C, 300°C, and 600°C temperatures. They studied the pre-heating and post-heating properties of functionally graded concrete with the replacement of NFA by crumbs of WTR up to 10%. The test results indicated that the three-layer concrete at equal steel fibre content possesses higher flexural properties followed by one- and two-layered concrete beams. Moreover, flexural properties increase for post-heating conditions at 300°C. While incorporating crumbs of WTR as fine aggregate decreases flexural properties by around 10% at 10% replacement. The performance of concrete worsens at the combination of 10% NFA replacement with the post-heating condition at 600°C. Based on flow rule and analytical analysis, Sabetifar et al. (2022) developed a model for studying concrete-filled steel tubes (CFST) containing steel fibre reinforcement up to 1.5% volume fraction and crumbs of WTR replacing NFA up to 10% levels under axial compressive load condition. They focused on estimating the load-bearing capacity of steel tubes, and hoop strain-axial strain relationship, and the axial stress-volumetric strain relationship of CFST for post-heating effects at 20°C, 250°C, 500°C, and 750°C temperature conditions.

It is observed that the processing of waste tyres in chipped and crumb form can produce granular and fibre-shaped rubber particles. Compared to granular shape, fibre-shaped WTR has been employed as additives similar to virgin fibres (As'ad et al. 2011; Hernández-Olivares et al. 2007; Hernández-Olivares and Barluenga 2004) and as aggregates in place of natural aggregates (Da Silva et al. 2015; Li et al. 2004a). Various research studies are available comparing the effectiveness of WTR's particle shape between granular and fibre for use as fine aggregates (Angelin et al. 2019; Li et al. 2004a, 2004b; Yilmaz and Degirmenci 2009). In the experimental investigations, Li et al. (2004a, 2004b) found that fibre-shaped WTR decreases workability compared to rubber chips. However, due to its effective load transfer mechanism, fibre-shaped WTR resulted in higher compressive strength and split tensile strength than rubber chips (Li et al. 2004a, 2004b). In another study, Yilmaz and Degirmenci (2009) reported better compressive strength and flexural strength of fibre-shaped WTR than granular-shaped WTR in the cementitious composite. In a study, Angelin et al. (2019) investigated the compressive strength, flexural

strength, and sound attenuation properties of rubberised mortar. They separately used granular and fibre-shaped WTR as fine aggregates up to 30% replacement levels. The study revealed that fibre-shaped WTR improves the compressive strength, flexural strength, and sound attenuation properties of rubberised mortar as compared to granular-shaped WTR (Angelin et al. 2019). The incorporation of fibre-shaped WTR provides a better load transfer mechanism due to particle elongation over granular-shaped WTR (Angelin et al. 2019; Li et al. 2004b). The post-failure interaction between rubber and surrounding cementitious paste remains higher due to the fibre shape of WTR, which is not possible in granular-shaped WTR (Li et al. 2004b). Therefore, the efficacy of rubberised cementitious mixes can be improved by fibre-shaped WTR's effective load transfer capacity and post-failure residual strength. Based on observed literature, the current study focuses on using fibre-shaped WTR as fine aggregates in cementitious mixes.

Furthermore, literature has been studied to understand the effect of WTR fibre on various properties of cementitious mixes. It is observed in the normally compacted concrete (NCC) that the WTR fibre improves the flexural strength (Gupta et al. 2014), fracture toughness (Hernández-Olivares et al. 2007), impact resistance (Gupta et al. 2015a, 2017b), and the tensile strength (Luhar et al. 2019) of concrete. Additionally, WTR fibre enhances the endurance and utility of concrete by increasing its resistance to abrasion (Gupta et al. 2015b), corrosion (Gupta et al. 2016), acid attack (Gupta et al. 2019), heat insulation (Aliabdo et al. 2015), and sound attenuation (Angelin et al. 2019). Despite improvements in the properties as mentioned above, WTR fibre reduces workability (Da Silva et al. 2015), compressive strength (Angelin et al. 2019; Bandarage and Sadeghian 2020; Bideci et al. 2017; Da Silva et al. 2015; Gupta et al. 2015b; Topçu and Demir 2007), static and dynamic modulus of elasticity (Bandarage and Sadeghian 2020; Gupta et al. 2014; Kaewunruen et al. 2017; Topçu and Demir 2007), fire resistance (Gupta et al. 2017a), and water permeability (Gupta et al. 2016) of cement-based mixes.

Researchers in the past (Aslani and Gedeon 2019; Turatsinze and Garros 2008) found that incorporating lightweight rubber particles in self-compacting concrete (SCC) can prevent compaction issues due to high flowing ability and compaction under the self-weight of SCC. However, limited research studies (Angelin et al. 2015, 2017a, 2017b, 2020; As'ad et al. 2011; Bideci et al. 2017; Güneyisi et al. 2016; Hilal 2017; Thakare et al. 2020a) are observed on SCC with WTR fibre. As'ad et al. (2011) reported that WTR fibre, used as an additive in SCC, provides better fresh properties such as flowing ability, filling ability, and passing ability. They reported the efficacy of fresh properties of SCC is improved for fine (diameter < 0.2 mm and length < 30 mm) WTR fibre size compared to coarse (diameter 2 mm and

length 20 mm) WTR fibre size. Güneyisi et al. (2016) studied the rheological performance of SCC with WTR fibre when used as fine and coarse aggregates separately. The replacement of granular fine and coarse aggregates individually by elongated rubber particles increased the torque of the mix at the low shear rate (Güneyisi et al. 2016). They also reported that fine aggregate replacement resulted in a lower loss in rheological properties such as yield stress and plastic viscosity compared to coarse aggregate replacement. In a study, Thakare et al. (2020a) found the improved rheological properties of self-compacting mortar (SCM) with WTR fibre up to 15% replacement of fine aggregate due to fibre flexibility.

In the experimental investigation, Angelin et al. (2015, 2017a, 2017b) demonstrated the effect of substituting fine aggregate with crumb rubber composed of 28% fibre and 72% granular particles, which restricted the understanding of the effect of rubber fibre on SCM characteristics. Bideci et al. (2017) reported concrete with WTR fibre as coarse aggregate with up to 15% replacement levels complied with the criteria for SCC as per EFNARC (2005) and improved the segregation resistance. They found increased fracture toughness with the decreased compressive strength of SCC with WTR fibre. In another study, Hilal (2017) reported that increasing WTR fibre content reduced the mechanical performance, such as compressive strength, flexural strength, indirect tensile strength, elastic modulus, and bond strength of SCC. The low stiffness of WTR fibre, the poor bond between fibre and cement paste, and the difference between the hardness of the original and replacing material, such reasons were reported for the decreased mechanical performance of SCC with WTR fibre (Hilal 2017). Angelin et al. (2020) reported a similar trend of decreased compressive strength and indirect tensile strength in self-compacting lightweight concrete. Among the existing literature, very few (As'ad et al. 2011; Bideci et al. 2017; Güneyisi et al. 2016; Thakare et al. 2020a) focused their research on investigating fresh properties, while limited studies (Angelin et al. 2015, 2017a, 2017b, 2020; Bideci et al. 2017; Güneyisi et al. 2016; Hilal 2017) have explored the hardened properties of SCC with WTR fibre.

It was observed in the literature that the incorporation of granular-shaped WTR in SCC improved the resistance against impact loading (AbdelAleem et al. 2018; Khalil et al. 2015; Li et al. 2019). Khalil et al. (2015) reported that using granular-shaped rubber particles as fine aggregate up to 40% replacement levels improved the impact resistance of SCC. They observed the highest impact strength of SCC with WTR at 30% replacement due to rubber's higher energy absorption capacity. In a study, AbdelAleem et al. (2018) reported that granular rubber particles increased the impact resistance of SCC by 91% for 30% replacement and 2.25 times for 25% replacement

under drop weight impact and flexural impact tests, respectively. They found that the rubber absorbed higher impact energy due to low stiffness, resulting in more impact blows required for failure. Moreover, the combined use of synthetic fibre-reinforcement along with rubber particles further enhanced the impact strength of SCC due to the bridging action of fibre (AbdelAleem et al. 2018). In another study, Li et al. (2019) observed the increase in size and content of granular-shaped rubber particles increased deformation capacity indicating higher ductility of SCC when examined under the split Hopkinson pressure bar impact test.

Similarly, the potential utilisation of fibre-shaped WTR particles to enhance the impact resistance of normally compacted concrete (NCC) has been explored in the past (Ataei 2016; Maho et al. 2019; Mhaya et al. 2021; Pham et al. 2018; Youssf et al. 2017). While in experimental investigations, Gupta et al. (2015a, 2017b) focused on evaluating the influence of variation in the WTR fibre content (0–25% replacements) on the impact and fatigue response of NCC. They reported the increased dynamic performance (impact and fatigue resistance) of NCC with WTR fibre at increasing replacement ratios (up to 25%) due to low stiffness and cracks encountering the fibre action of rubber particles. In another study, Gupta et al. (2021a, b) reported superior static and impact resistance properties of NCC with WTR fibre compared to NCC with rubber ash. They found that variation in size, shape, and content of rubber particles significantly altered the energy absorption of NCC.

Based on the literature review, it was found that the impact resistance of SCC using WTR fibre as a partial replacement of fine aggregate has not been explored. The influence of different sizes of WTR fibre on the static and impact resistance of cement-based mixes is also missing in the literature. Motivated by this, the current study was focused on investigating the static and impact load response of SCC containing different sizes of WTR fibre. Natural fine aggregate (NFA) was replaced by WTR fibre of three different sizes individually (0.60–1.18 mm, 1.18–2.36 mm, and 2.36–4.75 mm) at 10%, 20%, and 30% replacement levels. The influence of incorporating WTR fibre on the fresh properties of SCC was examined by the slump flow and sieve segregation tests. The scanning electron microscope (SEM) analysis has been executed on hardened samples of SCC with WTR fibre to understand their microstructural characteristics. For SCC with WTR fibre, the static load response was evaluated by the compressive strength and static modulus of elasticity (MOE) tests. The ductility of SCC with WTR fibre has been studied by the impact load resistance tests, i.e., rebound impact and drop weight impact. Other important properties such as density, water

permeability, and dynamic MOE tests have been performed on SCC with different sizes of WTR fibre. Relationships between dynamic MOE and impact tests (drop-weight impact and rebound impact test, separately) and the relationship between drop weight and rebound impact tests have been examined too. Moreover, the Weibull two-parameter distribution analysis has been used for statistical analysis of the drop weight impact test.

## Research significance

For environment-friendly construction practices, the disturbance to the natural resources must be prevented, or their utilisation must be lowered while developing the construction products. The production of natural fine aggregates, i.e., river sand and crushed stones, deteriorates the natural resources and pollutes the environment. In the context of reducing the use of NFA in cementitious mixes, it is imperative using alternate materials.

The automobile industry is creating an environmental concern by scraping a large number of waste rubber tyres around the globe. Over a year, China produces 14.5 million tons, the USA produces 3.7 million tons, Europe produces 3.4 million tons, and India produces 2.7 million tons of waste tyres (Recycling magazine 2020, WBCSD & The Tire Industry Project 2019). The massive amount of waste tyres create disposal issues due to their non-biodegradable nature. Conventional disposal methods (landfilling, stockpiling, incineration, and converting into fuels) and recycling into domestic and industrial products are not enough to safely dispose of the considerable quantity of waste tyres (Ba Thai et al. 2019). Therefore, the researchers explore the various disposal alternatives such as embankment filler, retaining structures, developing artificial reefs, use in the steelmaking process, and use in cementitious mixes (Callinan and Cashman 2005, Mohajerani et al. 2020, Raghavan et al. 1998, Zaharia et al. 2009). Among the various disposal alternatives, using WTR in cementitious mixes is one of the safe, environment-friendly, and cost-efficient disposal methods (Thomas and Gupta 2016). Moreover, practising WTR as an alternate constituent of concrete could partially relieve the burden on natural resources to produce natural fine aggregate. Thus, dual benefits of safe waste disposal and partial relief to the natural resources can be availed by using WTR as fine aggregate in cementitious mixes.

It has been observed that waste tyres are processed by mechanical, pyrolysis, or cryogenic processes for the recycling industries (Thomas and Gupta 2016). The processing of waste tyres yields various sizes and shapes of WTR particles. After visiting the recycling industries, it

is noticed that the obtained WTR particles are segregated, and particles less than 0.60 mm in size are supplied to the recycling industry by the waste tyre processing industry. While subsequent industries do not prefer WTR particles greater than 0.60 mm sizes and thus re-processing of coarser WTR particles ( $> 0.60$  mm) is needed. The re-processing of WTR particles greater than 0.60 mm in size is uneconomical and consumes higher energy. Therefore, using WTR particles greater than 0.60 mm in cementitious mixes can be promoted for economic and environment-friendly benefits. In the present research, WTR particles greater than 0.60 mm size further segregated into three different sizes of 0.60–1.18 mm, 1.18–2.36 mm, and 2.36–4.75 mm to better understand the effect of particle size variation of WTR as fine aggregate in self-compacting concrete (SCC).

The processing of waste tyres produces granular and fibre-shaped WTR, which can be used as fine aggregate in cementitious mixes. Among WTR's granular and fibre shapes, researchers (Angelin et al. 2019; Li et al. 2004a, 2004b; Yilmaz and Degirmenci 2009) suggest the use of fibre-shaped WTR as a fine aggregate over granular-shaped WTR for improved efficacy of rubberised cementitious mixes. Therefore, this study aimed to investigate the effect of varying sizes of fibre-shaped WTR as fine aggregate on the properties of SCC.

The use of WTR fibre as fine aggregate has been investigated in the past (Al-Hadithi and Hilal 2016; Gupta et al. 2014; Yilmaz and Degirmenci 2009), which revealed that the addition of fibre-shaped WTR may decrease some of the important structural properties of concrete such as compressive strength, flexural strength, and split tensile strength. On the other hand, increment in

granular-shaped WTR content as fine aggregate improves concrete's impact resistance due to the high flexibility of rubber particles (AbdelAleem et al. 2018; Khalil et al. 2015; Li et al. 2019), which is imperative to be evaluated for fibre-shaped WTR particles in SCC. Therefore, in this study, fresh, static load and ductility properties are evaluated using various sizes of WTR fibre as fine aggregate in SCC.

The results of the present study will be helpful in understanding the effects of size and replacement ratio variations on static load and ductility properties of SCC. This study will encourage researchers, industry persons, and design consultants to account for the available onsite sizes of WTR fibre for field implementation. The results of the present study can justify the concrete's use for high ductility applications along with the replacement of NFA with WTR fibre as environment-friendly construction practice.

## Experimental programme

### Materials, mix proportioning and casting

In the present study, SCC with WTR fibre was prepared using ordinary Portland cement (OPC) of 43 grade confirming BIS 8112 (2013) and coal-based fly ash (FA) confirming BIS 3812 (2013). Crushed stones were used as natural fine aggregate (NFA) with particle size  $\leq 4.75$  mm and natural coarse aggregate (NCA) comprising particle size between 4.75 and 12.5 mm. NFA and NCA, with a specific gravity of 2.92 and 2.85, were found to have a water absorption of 2.32% and 1.74%, respectively. The desired workability of concrete was

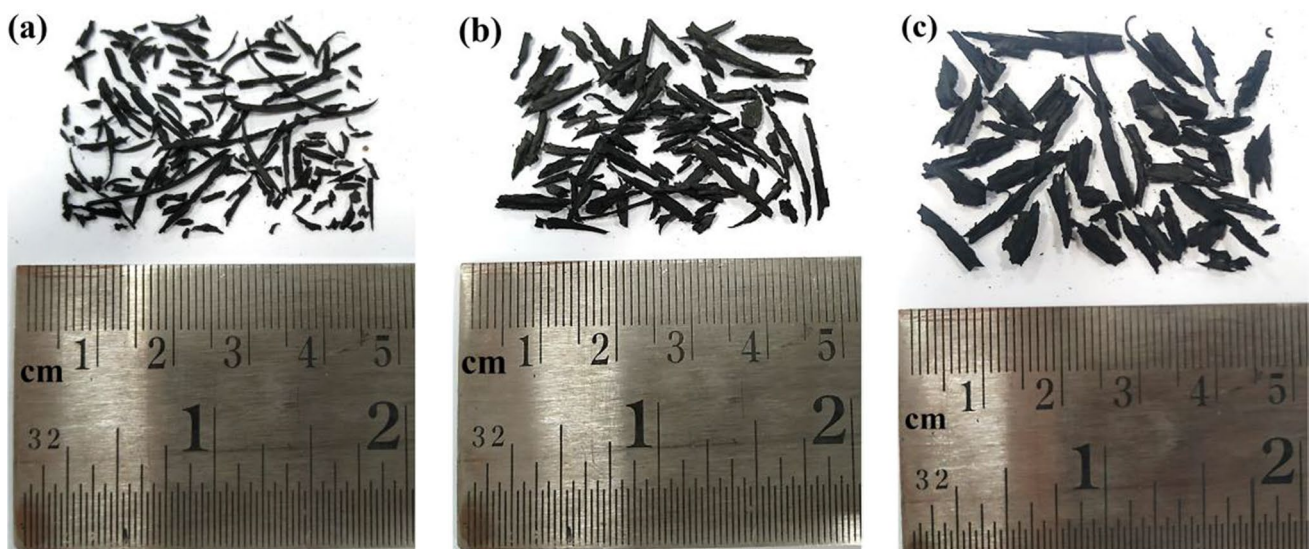


**Fig. 1** Varying sizes of waste tyre rubber fibre **a** 0.60–1.18 mm, (fine), **b** 1.18–2.36 mm (medium), **c** 2.36–4.75 mm (coarse)

obtained by adjusting the dose of superplasticiser (SP) named Glenium SKY 8777 (make: BASF). The normal tap water was used for concrete mixing and curing purposes. The available mixed-size WTR fibre was collected from the local waste tyre industry. Then WTR fibre was segregated into 0.60–1.18 mm (fine), 1.18–2.36 mm (medium), and 2.36–4.75 mm (coarse) sizes, as shown in Fig. 1a–c. The fibre-shaped WTR has been used as fine aggregate in SCC up to 30% replacement levels. Table 1 depicts the proportion of materials used.

The material composition of the control mix (SCC without WTR fibre) was determined by following the mix design approach prescribed in EFNARC (2005), designated as CON. The SCC mixes with WTR fibre are designated as shown in Table 1. The labelling of mixes was done in the following order; the first alphabet represents the size of the WTR fibre (F, fine; M, medium; C, coarse), next two digits represent the WTR fibre replacement ratio with NFA (10%, 20%, and 30%).

All SCC mixes with and without WTR fibre were prepared using a tilting drum-type rotary mixer with a 210-s mixing period. A dry-to-wet mixing strategy was used to accomplish homogeneous blending of the concrete mix in each batch, as illustrated in Table 2. The natural aggregate with a saturated surface dry (SSD) was employed.

## Testing methods

Sieve segregation and slump flow experiments were performed to evaluate the fresh state performance of SCC with WTR fibre, representing its stability and mobility according to EFNARC (2005). The microstructural properties were studied on a  $10 \times 10 \times 9$  mm concrete sample using SEM model Nova Nano FE-SEM 450. SCC with WTR fibre's compressive strength and density were evaluated using a  $100 \times 100 \times 100$  mm cube following BIS 516 (2004) and ASTM C 642 (2013), respectively.

The water resisting capacity of concrete mixes was determined by performing a water permeability test on the cube of  $150 \times 150 \times 150$  mm as per DIN 1048 (Part 5 1991). The concrete specimens were oven-dried at  $60^\circ\text{C}$  for 5 days and then kept under the constant water pressure of  $0.5 \text{ N/mm}^2$  for 72 h. The concrete specimen was then split into two halves, and the depth of water penetration was measured in mm as per DIN 1048 (Part 5 1991).

The static modulus of elasticity (MOE) was determined using a cylinder with a diameter of 150 mm and a height of 300 mm following ASTM C 469 (2002). The specimen's load capacity and related strains were recorded. SCC with WTR fibre's modulus of elasticity was determined using Eq. (1).

**Table 1** Mix proportions of self-compacting concrete with waste tyre rubber fibre ( $\text{kg/m}^3$ )

Mix ID	Cement ( $\text{kg/m}^3$ )	Fly ash	NFA	WTR fibre	NCA	Water	SP ( $\%1$ )
CON	402.50	172.50	894.88	0.00	787.67	201.25	0.20
F10	402.50	172.50	805.39	34.32	787.67	201.25	0.18
F20	402.50	172.50	715.90	68.65	787.67	201.25	0.20
F30	402.50	172.50	626.42	102.97	787.67	201.25	0.25
M10	402.50	172.50	805.39	34.32	787.67	201.25	0.19
M20	402.50	172.50	715.90	68.65	787.67	201.25	0.23
M30	402.50	172.50	626.42	102.97	787.67	201.25	0.27
C10	402.50	172.50	805.39	34.32	787.67	201.25	0.21
C20	402.50	172.50	715.90	68.65	787.67	201.25	0.25
C30	402.50	172.50	626.42	102.97	787.67	201.25	0.30

<sup>1</sup>weight percentage of total binder; NFA, natural fine aggregates; WTR, waste tyre rubber; NCA, natural coarse aggregates; SP, superplasticizer

**Table 2** Mixing protocol for self-compacting concrete with waste tyre rubber fibre

Stages	Mix description	Mixing period
I	Dry mixing of aggregate (coarse, fine, and WTR fibre)	30 s
II	Addition and mixing of cement and fly ash for uniform blending	30 s
III	Addition of 50% of the total water and during continuous mixing	60 s
IV	Mixing of remaining 50% of total water and superplasticizer together and added during continuous mixing	90 s

$$\text{Static modulus of elasticity} = \frac{\sigma_1 - \sigma_2}{\epsilon_2 - 0.000050} \tag{1}$$

where  $\sigma_1$ , stress concerning an axial strain of 50 millionths ( $\epsilon_1$ );  $\sigma_2$ , stress concerning 40% of ultimate load, and  $\epsilon_2$ , axial strain produced by  $\sigma_2$ .

Dynamic MOE was determined by performing an ultrasonic pulse velocity (UPV) test as per BIS 13311(1992) on the cube of  $150 \times 150 \times 150$  mm. The UPV values were used to compute the dynamic MOE using Eq. (2) given by Gupta et al. (2016).

$$\text{Dynamic modulus of elasticity} = \frac{V^2 \cdot \rho}{g \times 100} \tag{2}$$

where  $V$ , ultrasonic pulse velocity (km/s);  $\rho$ , density of concrete ( $\text{kg/m}^3$ );  $g$ , acceleration due to gravity ( $9.81 \text{ m/s}^2$ ).

The ductility is measured by performing rebound impact and drop weight impact tests on concrete specimens. The  $150 \times 150 \times 150$  mm cube was used to conduct the rebound impact test. The test was performed by dropping a steel ball of 0.25 kg weight on the specimen from 1 m height, and the ball rebound was recorded using a speed-sensitive camera. The potential energy at 1 m height and rebound height is denoted by  $I_{p1,r}$ , Eq. (3), and  $I_{p2,r}$ , Eq. (4), respectively. The difference between potential energy  $p_1$  and  $p_2$  is the total rebound impact energy ( $I_{t,r}$ ). The air resistance was neglected.

$$I_{p1,r} = m \times g \times h_1 \tag{3}$$

$$I_{p2,r} = m \times g \times h_2 \tag{4}$$

where  $m$ , weight of steel ball (0.25 kg);  $g$ , gravitational acceleration ( $9.81 \text{ m/s}^2$ );  $h_1$ , ball height at the first position (1 m);  $h_2$ , ball height observed after rebound (different heights obtained for various mixes in m).

A drop weight impact test was conducted on a circular disk with a diameter of 150 mm and a thickness of 65 mm to assess the impact resistance/energy absorption of SCC with WTR fibre according to ACI 544(1999). The test equipment used is shown in Fig. 2. The number of impacts ( $N_1$ ) required to cause a first fracture in the top surface and the successive number of impacts ( $N_2$ ) required to cause ultimate failure (widening of the crack) was determined under repeated drop loads. Notations  $I_{f,dw}$ , Eq. (5), and  $I_{u,dw}$ , Eq. (6) signify the drop weight impact energy at the first crack and the final crack, respectively.

$$I_{f,dw} = N_1 \times m \times g \times h \tag{5}$$

$$I_{u,dw} = N_2 \times m \times g \times h \tag{6}$$



Fig. 2 Drop weight impact test setup

where  $N_1$ , number of impacts generating the first crack;  $N_2$ , number of impacts imparting ultimate failure;  $m$ , weight of the standard compaction hammer (4.54 kg);  $g$ , gravitational acceleration ( $9.81 \text{ m/s}^2$ );  $h$ , hammer drop height (457 mm).

## Results and discussions

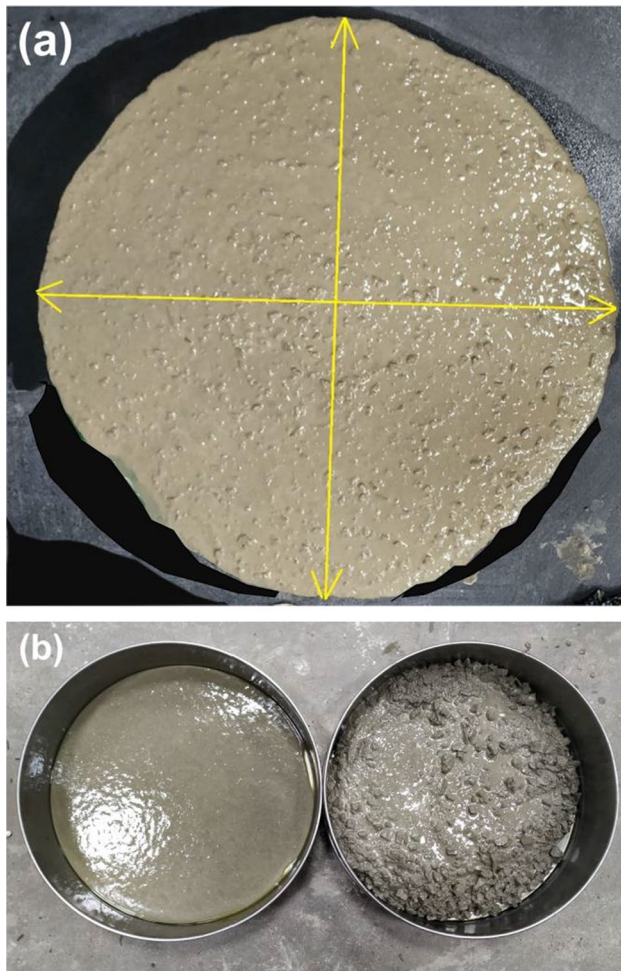
### Fresh properties

#### Slump spread and segregation resistance

The stability and mobility of SCC with WTR fibre in the fresh condition were determined using sieve segregation resistance and slump flow, respectively, and the findings are shown in Table 3. Figure 3a depicts the slump flow of F10. According to EFNARC (2005), SCC mixes CON, F10, F20, F30, M10, M20, and C10 reached slump flow class SF2 with a bit of adjustment in SP content, whereas M30, C20, and C30 fall into the SF1 group (EFNARC 2005). It was noticed that when the percentage of WTR fibre replacement increased, the SP content rose for each fibre size (Table 2). Despite increased SP content, slump

**Table 3** Slump spread and sieve segregation resistance of self-compacting concrete with waste tyre rubber fibre

Mix ID	CON	F10	F20	F30	M10	M20	M30	C10	C20	C30
SF (mm)	722	703	690	687	710	676	633	678	628	579
SS (%)	14.50	14.16	11.60	9.08	13.28	10.83	7.15	11.56	9.88	4.76

**Fig. 3** Fresh properties of concrete mixes — **a** slump flow of F10, **b** sieve segregation of C10

flow was lowered at each increment level of WTR fibre for the same fibre size. The slump flow reduction may be ascribed to the roughness or jagged surface of the rubber particle, which increases the inter-particle friction between the fibre and cementitious paste (Angelin et al. 2015; Reda Taha et al. 2008). Another reason for the reduced slump flow is the fibre form of rubber particles, which restricts particle mobility due to the interlocking effect (Aïssoun et al. 2016).

The variation in the fibre size has a considerable effect on the slump flow of concrete at each replacement level. Concrete with fine WTR fibre showed better flowing ability than medium and coarse concrete. The superior slump flow

of fine WTR fibre over medium and coarse fibre may be attributed to fine fibre's ability to move through aggregate inter-spaces (As'ad et al. 2011). Dominantly, the mechanical interaction between the fibre and the natural aggregate might have reduced the flow spread of medium and coarse WTR fibres (Thakare et al. 2020a). In a study, As'ad et al. (2011) used two different sizes of WTR fibre, i.e., a fine tyre of a diameter < 0.20 mm and length < 30 mm and a coarse tyre with a diameter of 2 mm and length of 20 mm, as an additive. They found that adding fine tyre fibre showed better slump flow than coarse tyre fibre. However, the increased fibre content decreased the slump flow of both sizes of WTR fibre. A similar effect of reduction in slump flow on the increased fibre content in rubberised SCC is observed in this study.

The stability of SCC with WTR fibre was quantified in terms of resistance to segregation, as illustrated in Fig. 3b. Segregation resistance was reported at a maximum of 4.76% and a minimum of 14.50% for mixes C30 and CON, respectively. According to EFNARC (2005), all SCC with WTR fibre mixes complies with segregation-resistant class SR2. The increased segregation resistance of SCC was found with increased fibre content for each fibre size can be associated with the elongated shape of rubber particles (Bideci et al. 2017). Due to the overlapping of fibres, a network structure may have evolved, which holds the concrete matrix together (Cao et al. 2016, 2018). As shown in Table 3, increasing fibre size improved the mix's segregation resistance at each replacement level. The superior segregation resistance of SCC for increased WTR fibre size can be attributed to the fibre being inter-particle locking with the aggregates (Thakare et al. 2020a). The impediment to aggregate separation posed by coarse WTR fibre was significantly greater than that of medium and fine fibre. The findings of this investigation corroborate those of Bideci et al. (2017). Bideci et al. (2017) incorporated WTR fibre of 5 mm cross-section with three different lengths of 25 mm, 50 mm, and 75 mm as coarse aggregate up to 15% replacement levels. They reported a maximum of 83.30% segregation resistance at a 10% replacement level for 25 mm length WTR fibre.

## Hardened properties

### Microstructural analysis

Microstructural analysis was performed on SCC with WTR fibre mixes, and the SEM images of F10, M10, and



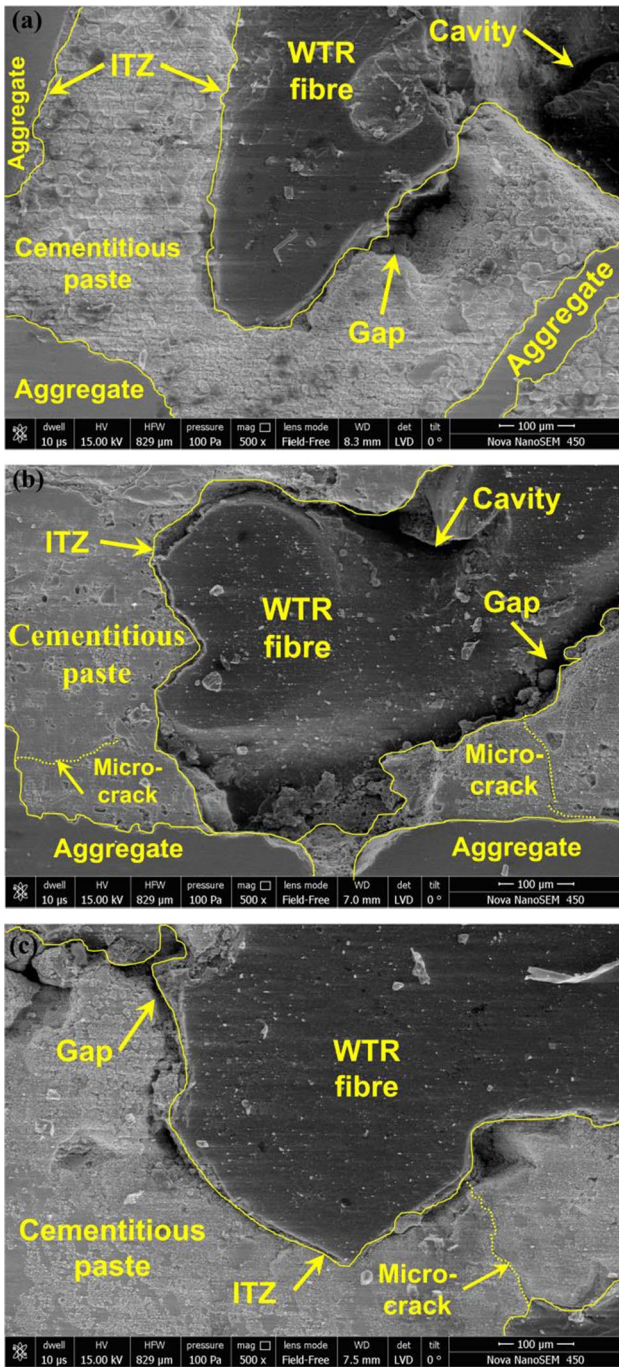


**Fig. 4** Micrograph of self-compacting concrete with waste tyre rubber fibre **a** micrograph of mix F10, **b** micrograph of mix M10, **c** micrograph of mix C10

C10 are shown in Fig. 4a, Fig. 4b, and Fig. 4c, respectively. The SEM image in Fig. 4a–c demonstrates the inadequate inter-particle connection between WTR fibre and cementitious paste in terms of the gap at the interfacial transition zone (ITZ). Because WTR fibre is hydrophobic, it has a tendency to hold air on its surface, which

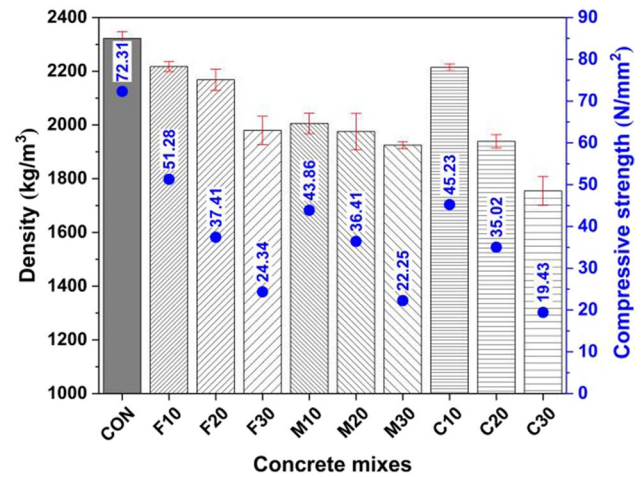


**Fig. 5** The density and compressive strength of self-compacting concrete with waste tyre rubber fibre

may be the primary explanation for the gap between rubber and cementitious paste at ITZ (Reda Taha et al. 2008). Rubber particles’ microstructural characteristics, such as cavities and microcracks, act as air pockets (Thakare et al. 2020a). Additionally, micro-voids and microcracks in the cementitious paste were discovered in the vicinity of rubber particles. As a result, the cumulative porosity of the mix increased with the addition of WTR fibre. Similar microstructural characteristics in the rubber incorporated cementitious mix were observed by Karakurt (2015) and Yeo et al. (2021). The variation in the sizes of WTR fibre has shown a comparable effect on the microstructure of concrete at ITZ. The poor interaction between rubber and cementitious paste and microcracks in the vicinity of rubber was visible for each size (fine, medium, and coarse) WTR fibre mix, as shown in Fig. 4a–c. The effect on the microstructure at ITZ is not significantly varied for WTR fibre’s size variation. However, the increased porosity caused by the addition of WTR fibre has considerable potential to alter the hardened properties of SCC (Angelin et al. 2015). The gap between fibre and cementitious paste can affect the load transfer mechanism within the matrix. The enhanced porosity in the concrete due to microcracks, micropores, and the cavity in the rubber fibre may affect the durability of the concrete (Gupta et al. 2019). In the experimental investigation, Gupta et al. (2019) observed the gap between rubber and surrounding cement paste. Moreover, a cavity in the cement paste and microcracks are also found in the microstructure of rubberised concrete. In a study, Karakurt (2015) observed micropores and microcracks in the vicinity of rubber due to the hydrophobicity of rubber. This study observes similar microstructural characteristics in the vicinity of WTR fibre.

## Density

The density fluctuation of different SCC with WTR fibre mixes is depicted in Fig. 5, and the error bar indicates the standard deviation. The highest and the lowest density was observed for the control (CON) and C30 mixes as  $2322.13 \text{ kg/m}^3$  and  $1754.37 \text{ kg/m}^3$ , respectively. As illustrated in Fig. 5, the inclusion of WTR fibre resulted in a decrease in the density of SCC with WTR fibre. The density of SCC with WTR fibre decreased by 4.51%, 6.62%, and 14.76% when F10, F20, and F30 mixes were tested; 13.63%, 14.94%, and 17.12% when M10, M20, and M30 mixes were tested; and 4.64%, 16.50%, and 24.45% when C10, C20, and C30 mixes were tested. SCC with WTR fibre's density decrease due to the substitution of relatively heavy material (NFA) by lightweight WTR fibre (Gupta et al. 2014; Khaloo et al. 2008). The NFA of specific gravity of 2.92 was replaced with WTR fibre with a specific gravity of 1.12, which resulted in a drop in concrete density. It was observed that rubber tends to entrap air around WTR fibre due to the rubber's hydrophobicity. Moreover, the morphological discontinuities in the microstructure of WTR fibre, such as jagged surfaces and microcracks, include empty spaces. Cumulatively, such might have increased the mix's air content, resulting in a decrease in the density of SCC with WTR fibre (Reda Taha et al. 2008). A significant change in the density of concrete has been observed by Gupta et al. (2014) while replacing the natural river sand with WTR fibre up to 25% replacement levels. They found the combined effect of induced porosity, improper compaction, and, most importantly, replacement of relatively heavier fine aggregate by lighter weight WTR fibre decreased the density of rubberised concrete.

As illustrated in Fig. 5, the size of WTR fibre substantially affected the rate of density reduction in SCC with WTR fibre. Compared to the control mix, the drop in density for fine fibre was the smallest, while the reduction in density for coarse fibre was the greatest. The variation in density reduction for varied-size fibre could be related to the amount of air trapped in the mix. Due to the development of pore spaces in the coarse, fibre mixes and the fibre overlapping may have significantly lowered the density of SCC with coarse fibre. The fine fibre may be due to its filling ability, resulting in a lesser fall in SCC with WTR fibre density. The findings of this investigation corroborate those of Aslani and Khan (2019).

## Compressive strength

The compressive strength of concrete was evaluated after 28 days of curing, and the findings are shown in Fig. 5. Compressive strengths of  $72.31 \text{ N/mm}^2$  and  $19.43 \text{ N/}$

$\text{mm}^2$  were recorded for mixes CON and C30, respectively. As illustrated in Fig. 5, replacing NFA with WTR fibre decreased the compressive strength for each fibre size. Additionally, the highest replacement amounts for each fibre size resulted in the highest decrease rate. The decrease in compressive strength can be attributed to (i) the addition of soft WTR particles in place of relatively hard NFA (Gupta et al. 2017a; Su et al. 2015), (ii) insufficient inter-particle connection between rubber and surrounding cementitious paste (Gupta et al. 2016; Reda Taha et al. 2008), and (iii) induced porosity caused by the hydrophobicity of rubber particles (Angelin et al. 2019; Ganjian et al. 2009; Na and Xi 2017). Incorporating soft rubber particles, which cannot transfer applied loads and act as a void in the mix, led to an insufficient load-carrying capacity of SCC with WTR fibre (Hilal 2017). Additionally, the weak inter-particle connection between the rubber and the surrounding cementitious paste works as a stress concentrator, propagating cracks in the cementitious paste (Hesami et al. 2016; Hilal 2017). From Fig. 4, the gap between rubber and cementitious paste was evidenced, which might have acted as the epicentre for the crack propagation in the concrete (Eldin and Senouci 1993). Furthermore, adding WTR fibre formed empty spaces in hardened concrete due to increased air content in the mix, which lowered its compressive strength (Gupta et al. 2016). The reduction in the compressive strength due to the incorporation of WTR fibre as fine aggregate is commonly observed in past studies (Gupta et al. 2016; Hilal 2017). Gupta et al. (2016) found a decrement in compressive strength of 52 up to 25% replacement of NFA by WTR fibre. Whereas Hilal (2017) observed around 35% reduction in compressive strength up to 25% replacement of NFA by WTR fibre in SCC.

The varied sizes of WTR fibre (fine, medium, and coarse) have influenced the compressive strength of SCC. At each replacement level, the rate of compressive strength loss was the lowest for fine fibre but rose as the fibre size increased. The most significant loss of compressive strength in coarse fibre may result from fibre clustering and a reduction in slump flow (Table 2). The movement of fine fibre between aggregate inter-spaces may have facilitated filling (As'ad et al. 2011), resulting in a higher compressive strength than that of medium and coarse fibre. The relationship between the compressive strength and density of SCC with WTR fibre was found using a regression analysis method based on the observation, as shown in Fig. 6. The data were analysed using linear curve fitting, resulting in correlation coefficients ( $R^2$ ) of 0.90, 0.94, and 0.88 for the fine, medium, and coarse fibre sizes. The correlation coefficient ( $R^2$ ) was found to be more than 0.70, indicating a strong

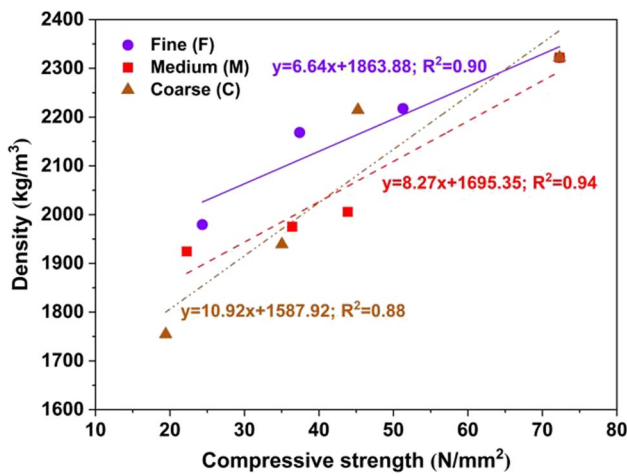


Fig. 6 Relation between compressive strength and density of self-compacting concrete with waste tyre rubber

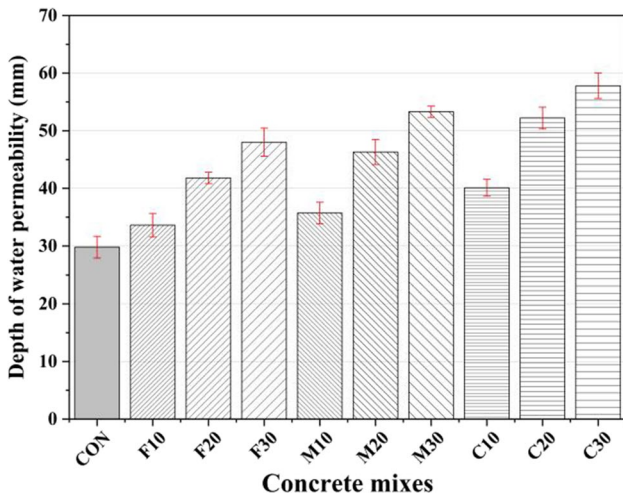


Fig. 7 Water permeability of self-compacting concrete with waste tyre rubber fibre

association between the compressive strength and density of SCC with WTR fibre.

**Water permeability**

The water permeability test was performed on various SCC mixes with WTR fibre, and the obtained results are depicted in Fig. 7. The nearest and the farthest depth of water penetration were recorded as 29.80 mm and 57.80 mm for CON and C30 mix, respectively. It was observed that the incorporation of WTR fibre increased the water penetration depth of the control mix. Compared to control mix, the depth of water penetration increased by 12.75%, 40.27%, and 61.07% for fine size fibre; 19.80%, 55.37%, and 78.86% for medium size

fibre; 34.56%, 75.17%, and 93.96% for coarse size fibre at 10%, 20%, and 30% replacement levels, respectively. The increased water permeability on the incorporation of WTR fibre indicated the increased porosity in the concrete (Ganjian et al. 2009). The incorporation of WTR fibre formed the pore spaces due to poor bonding between WTR fibre and cement paste. The gap between rubber and cementitious paste and microcracks in the mix might have acted as permeable conduits for water penetration (Thakare et al. 2022b). Although the rubber tends to repel the water due to its hydrophobicity, the pores present in the vicinity of the rubber filled with the water might be due to the applied constant water pressure during the test (Ganjian et al. 2009). The results of the increase in the water permeability of concrete on incorporating WTR fibre are in line with the previous study (Gupta et al. 2016). The water permeability was found to increase for each fibre content with the increased WTR fibre size. The increased water permeability for coarse size represents more pore spaces in the mix (Gesoğlu et al. 2014). The fine size might have filled the gaps between coarse aggregates resulting in lower water permeability than medium and coarse fibre (Gesoğlu et al. 2014). In a study, Ganjian et al. (2009) found an increase in depth of water permeability from around 14 mm for control mix up to 35 mm for rubberised at 10% replacement of natural coarse aggregate. In another study, Gupta et al. (2016) reported around a 30% increment in the water permeability due to the replacement of NFA by WTR fibre up to 25% replacement levels. The increment in the water permeability is attributed to the weak bond between the rubber and the surrounding cement paste (Gupta et al. 2016).

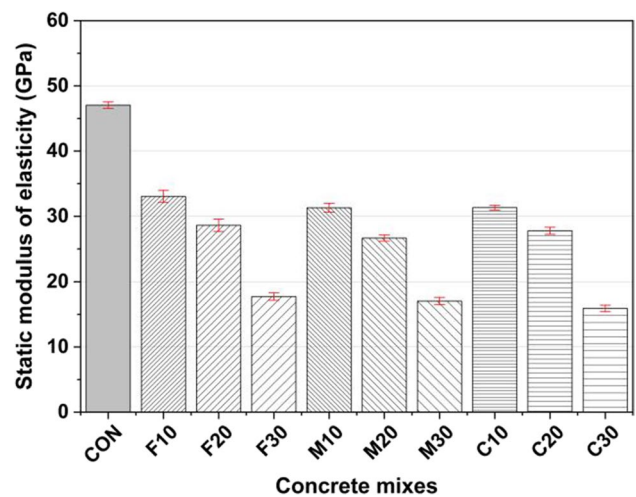
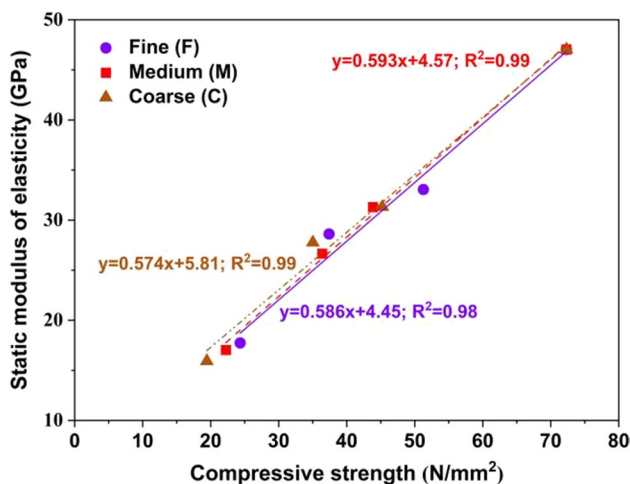


Fig. 8 Static modulus of elasticity of self-compacting concrete with waste tyre rubber fibre

## Static modulus of elasticity

Figure 8 illustrates the results of a static MOE test on various SCC with WTR fibre mixes. Control and C30 mixes have the highest elastic modulus of 47.04 GPa and the lowest elastic modulus of 15.92 GPa. As illustrated in Fig. 8, the static MOE of SCC with WTR fibre dropped as the WTR fibre concentration increased for each fibre size. The static MOE of control mix was reduced by 29.73%, 39.18%, and 62.31% for the fine fibre size; 33.48%, 43.35%, and 63.79% for the medium fibre size; and 33.42%, 40.97%, and 66.16% for the coarse fibre size at 10%, 20%, and 30% replacement levels, respectively. The observed decrease in static MOE is consistent with previous findings (Güneyisi et al. 2004; Gupta et al. 2016; Hilal 2017). The decrease in static MOE corresponded to the decrease in SCC with WTR fibre stiffness due to the addition of WTR fibre. The stiffness of concrete depends upon the hardness of the cementitious paste and the aggregate used. By substituting relatively soft material (WTR fibre) for NFA, the stiffness of the cementitious matrix (cementitious paste and fine aggregate) in SCC with WTR fibre was lowered. Due to higher deformation of low stiffened material, SCC with WTR fibre has improved deformability (Gupta et al. 2016). Another reason for the decrease in static MOE may be related to a weak inter-particle connection between the WTR fibre and cementitious paste at the interfacial transition zone (ITZ). Moreover, due to the addition of WTR fibre, the porosity in the concrete mix might have increased, resulting in lower strength (Hilal 2017). In a study, Hilal (2017) used 1–4 mm size WTR fibre as fine aggregate in SCC, which resulted in up to 36% reduction in static MOE due to the low stiffness of rubber replacing hard NFA. The high flexibility of rubber caused high deformability under the applied load, which further



**Fig. 9** Relation between compressive strength and static modulus of elasticity

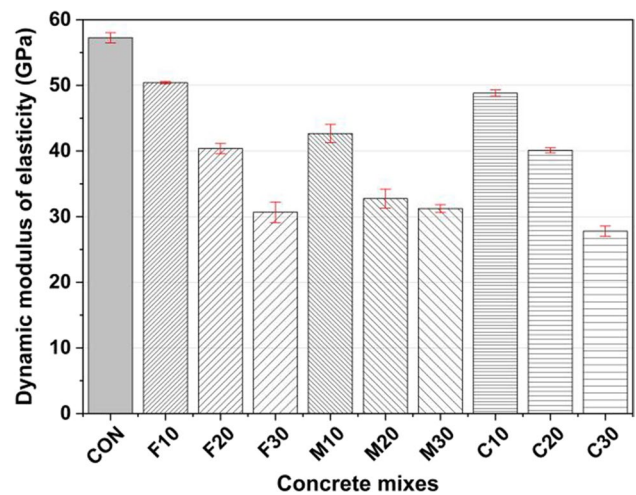


**Fig. 10** Dynamic modulus of elasticity of self-compacting concrete with waste tyre rubber fibre

led to a decrement in the static MOE of rubberised SCC (Hilal 2017).

Increased WTR fibre size resulted in a considerable decrease in static MOE for each replacement level. Thus, even with varying WTR fibre sizes, the brittleness of SCC with WTR fibre can be mitigated. The relationship between the compressive strength and static MOE of SCC with WTR fibre is depicted in Fig. 9. Similar to the drop in compressive strength, the incorporation of WTR fibre decreases static MOE. Compressive strength and static MOE are highly associated, with  $R^2$  values greater than 0.95 for each mix series (Fig. 9).

## Dynamic modulus of elasticity

SCC with WTR fibre's dynamic MOE is calculated using ultrasonic pulse transmission and density data. Figure 10 illustrates the dynamic MOE investigated in this study. When compared to control mix, dynamic MOE was reduced by 11.94%, 29.49%, and 46.45% for the fine fibre size; 25.50%, 42.79%, and 45.47% for the medium fibre size; and 14.73%, 29.96%, and 51.46% for the coarse fibre size at 10%, 20%, and 30% replacement levels respectively. The dynamic MOE is majorly affected by the partial substitution of WTR fibre with NFA. Incorporating WTR fibre resulted in material property non-uniformity lowering the UPV of SCC with WTR fibre (Hesami et al. 2016). Another possible explanation for the decreased dynamic MOE may be the rubber particles' energy dissipation property (Herrero et al. 2013). Additionally, the decrease in dynamic MOE is attributable to the drop in density caused by the higher porosity in SCC with WTR fibre (Marie 2016). Similar reductions in dynamic MOE due to the integration of rubber particles have been seen in the current literature (Gupta

et al. 2016; Rahman et al. 2012). In a study, Uygunoğlu et al. (2010) incorporated granular WTR as fine aggregate up to 50% replacement levels and determined the dynamic MOE of rubberised concrete. They reported a maximum of 68% reduction in dynamic MOE at a 50% replacement level for a 0.51 water-to-powder ratio. The increased porous structure and change in the material properties of the concrete matrix due to rubber incorporation caused a significant reduction in dynamic MOE (Uygunoğlu and Topçu 2010). In an experimental investigation, Gupta et al. (2016) reported a decrease in dynamic MOE of 52% for 25% replacement of NFA in rubberised concrete. The reduction in the dynamic MOE of rubberised concrete is reported as a positive gain for the implementation of concrete for its ductility requirements instead of strength requirements (Gupta et al. 2016).

The fine fibre size for each replacement level showed a lesser dynamic MOE reduction than medium and coarse fibre. Due to the generated porosity in the mix, the increasing size of WTR fibre dramatically affected the density of SCC with WTR fibre. The increased porosity of SCC with coarse fibre can be attributed to the lower slump flow caused by the fibre clustering effect. The significant disparity in dynamic MOE reduction for coarse fibre over fine and medium fibre may be related to the coarse fibre SCC with WTR fibre mixes' low density.

**Rebound impact energy**

The rebound impact energy is defined as the difference between the potential energy at 1 m above the specimen surface and the rebound height of a steel ball on concrete specimens. As shown in Fig. 11, the rebound impact energy of SCC increased with the addition of WTR fibre. SCC with WTR fibre's rebound impact energy increased

by 12.67%, 16.29%, and 22.85% for fine fibre; 9.50%, 13.80%, and 20.14% for medium fibre; and 6.79%, 9.73%, and 14.48% for coarse fibre at 10%, 20%, or 30% replacement levels, respectively. The increased rebound impact of energy on the increased content of WTR fibre was also seen in previous research studies by Abdelmonem et al. (2019) and Gupta et al. (2015b, 2017b). The enhanced flexibility of the cementitious matrix caused by the insertion of WTR fibre in SCC may result in an increase in energy absorption. The substitution of WTR fibre for NFA decreased the hardness of the cementitious matrix due to rubber particles' softness (Abdelmonem et al. 2019). Abdelmonem et al. (2019) investigated the effect of NFA replacement by granular WTR up to 30% replacement levels on the rebound impact resistance of rubberised concrete. They reported of 12% increased in impact resistance of rubberised concrete due to the energy absorption capacity of WTR in the concrete matrix (Abdelmonem et al. 2019). In multiple experimental studies, Gupta et al. (2015a, 2017b) found that using WTR in fibre form improved the rebound impact resistance of rubberised concrete. The trend in rebound energy absorption with respect to the size of WTR fibre is comparable to the variation in drop weight impact energy absorption.

The relationship between dynamic MOE and the rebound impact energy is depicted in Fig. 12. Correlation coefficients ( $R^2$ ) of 0.99 for fine fibre size, 0.99 for medium fibre size, and 0.99 for coarse fibre size indicated a high link between dynamic MOE and rebound impact energy. As a result, it can be noted that the increased impact energy of SCC with WTR fibre is due to the decrease in dynamic MOE. The addition of WTR fibre decreased the stiffness of the mix, increasing SCC with WTR fibre's energy absorption capacity.

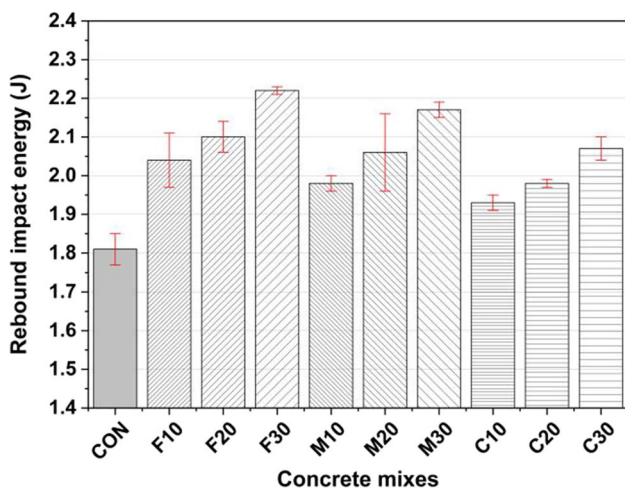


Fig. 11 Rebound impact energy of self-compacting concrete with waste tyre rubber fibre

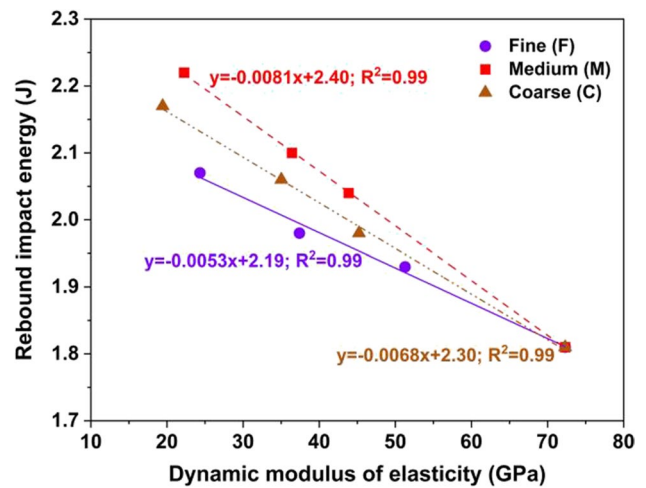


Fig. 12 Relation between dynamic modulus of elasticity and rebound impact energy

**Table 4** Drop weight impact energy of self-compacting concrete with waste tyre rubber fibre

Mix ID	$N_1$ (nos.)		$N_2$ (nos.)		$N_2 - N_1$ (nos.)	$I_{f,dw}$ (J)		$I_{u,dw}$ (J)		Post-crack capacity (%)
	Avg	SD	Avg	SD		Avg	SD	Avg	SD	
CON	86	4	102	3	16	1750	72	2069	67	18.22
F10	122	3	143	4	24	2483	60	2904	79	16.94
F20	194	2	226	3	32	3942	51	4607	67	16.87
F30	291	3	338	3	47	5930	69	6880	60	16.02
M10	112	4	130	4	18	2273	75	2653	75	16.72
M20	154	4	189	3	35	3141	79	3840	67	22.25
M30	283	3	323	2	40	5760	60	6581	51	14.25
C10	101	3	115	3	14	2062	58	2334	58	13.16
C20	162	3	187	3	25	3304	67	3813	67	15.40
C30	228	3	265	3	37	4634	69	5394	66	16.40

Avg., average; *SD*, standard deviation; *nos.*, numbers; *J*, Joule;  $I_{f,dw}$ , impact energy at first crack;  $I_{u,dw}$ , impact energy at ultimate failure

### Drop weight impact energy

The results of the drop weight impact test for various SCC mixes with WTR fibre are shown in Table 4. The impact energy at the first crack ( $I_{f,dw}$ ) and ultimate failure ( $I_{u,dw}$ ) was the number of impacts required to create an initial crack and ultimate failure, respectively. The control mix (CON) also had the fewest impacts at the initial crack and eventual failure, resulting in the lowest impact energy (Table 4). Adding WTR fibre enhanced the number of impacts for each fibre size. Additionally, when WTR fibre content increased, the difference between the number of hits for the first crack and ultimate failure ( $N_2 - N_1$ ) increased. The impact energy,  $I_{f,dw}$  was increased by 41.86%, 125.19%, and 238.76% for fine fibre size; 29.84%, 79.46%, and 229.07% for medium fibre size; and 17.83%, 88.76%, and 164.73% for coarse fibre size mixes at 10%, 20%, and 30% of control mix, respectively. The impact energy,  $I_{u,dw}$  concerning control mix was increased by 40.33%, 122.62%, and 232.46% for the fine fibre size; 28.20%, 85.57%, and 218.03% for the medium fibre size; and 12.79%, 84.26%, and 160.66% for the coarse fibre size at 10%, 20%, and 30% replacement levels, respectively. The substitution of WTR fibre for NFA decreased the stiffness of SCC with WTR fibre due to the flexible nature of rubber particles (Abdelmonem et al. 2019). The addition of WTR fibre increased the overall flexibility of the cementitious matrix (paste and fine aggregate) in SCC, hence increasing the energy absorption capacity even further. Another possible explanation for the increased impact energy is the fibre shape of the rubber particles that adhere to the broken surfaces (Gupta et al. 2015a). The impact load originates the fracture in the cementitious paste, which propagates as the number of impacts increases. However, the WTR fibre halted propagating cracks in the cementitious matrix, increasing the fracture toughness of SCC with WTR fibre (Thakare et al. 2022b). It is observed in research

studies conducted by Gupta et al. (2015a, 2017b) that the use of WTR fibre as fine aggregate up to 25% replacement levels increased the impact resistance of rubberised concrete by 4.5 times of the control mix. They found the replacement of cement with silica fume up to 10% further improved the efficacy of rubberised concrete (Gupta et al. 2015a).

When various sizes of WTR fibre were compared at the same replacement level, it was discovered that fine fibre absorbed the most energy, followed by medium and, lastly, coarse fibre (Table 4). Additionally, it can be noticed that the specimen's capacity to tolerate ultimate failure after the initial fracture ( $N_2 - N_1$ ) was more significant for the fine fibre size than for the medium and coarse fibre sizes. It should be noted that the fine fibre may result from its superior filling ability when uniformly dispersed throughout the mix. However, a higher size of WTR fibre resulted in the mix containing many empty spaces (Aslani and Khan 2019), which may have contributed to the lower energy absorption than fine fibre. The failure pattern of the specimens after performing a drop weight impact test for the control and F20 mix is shown in Fig. 13a and b, respectively. The difference in the failure pattern can be seen in the appearance of wide fractures in Fig. 13a for the control mix, compared to the formation of multiple narrow cracks visible in Fig. 13b for the F20 mix. The failure pattern presented decreased brittleness in SCC due to incorporating WTR fibre (Ismail and Hassan 2017). In general, the size and content of WTR fibre considerably increase the energy absorption capacity of SCC, which may encourage the use of WTR fibre in impact-resistant constructions.

The association between dynamic MOE and drop weight impact energy determined using linear regression analysis is depicted in Fig. 14. As illustrated in Fig. 14, the correlation coefficients ( $R^2$ ) are greater than 0.70, i.e., 0.73 for fine fibre sizes, 0.82 for medium fibre sizes, and 0.90 for coarse fibre sizes, indicating that the relationship

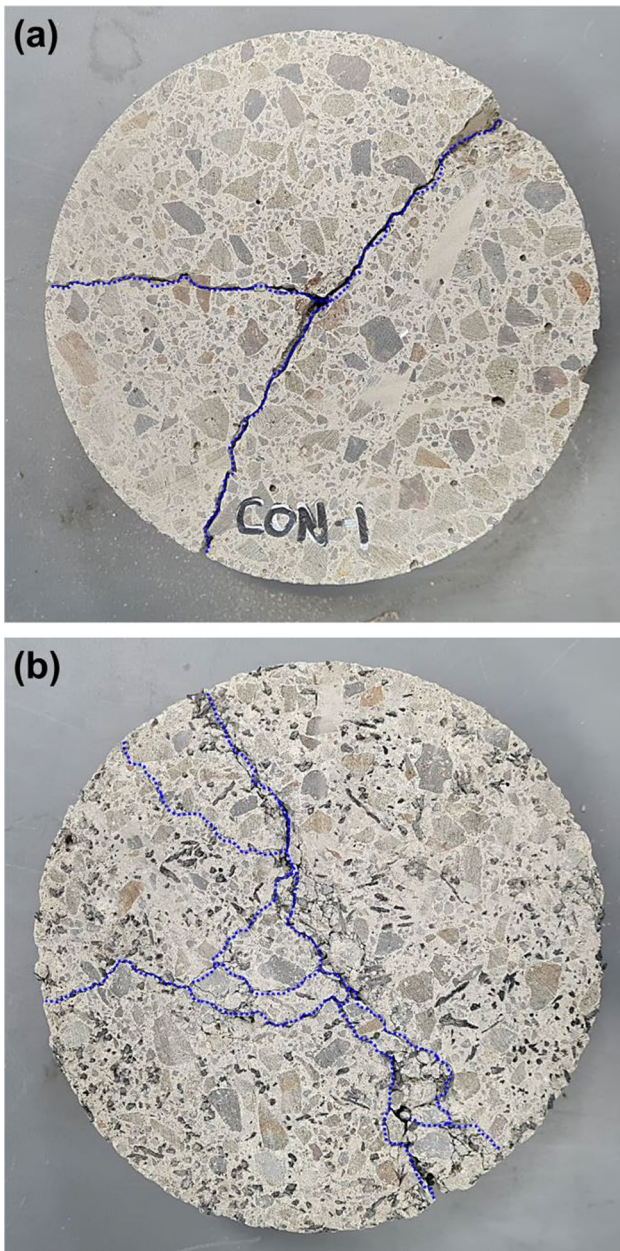


**Fig. 13** Failure pattern of the specimen under drop weight test **a** CON, **b** F20

equation is a reasonable model. Similarly, the regression analysis method was used to analyse the link between the rebound impact and drop weight impact energy of SCC with WTR fibre. As illustrated in Fig. 15, the linear link between these two qualities is widely established. Correlation coefficients ( $R^2$ ) of 0.83, 0.80, and 0.87 for the fine, medium, and coarse fibre sizes, respectively, indicate a decent link between rebound impact and drop weight impact energy.

Various probability distribution methods were recommended to analyse the impact resistance of cement-based

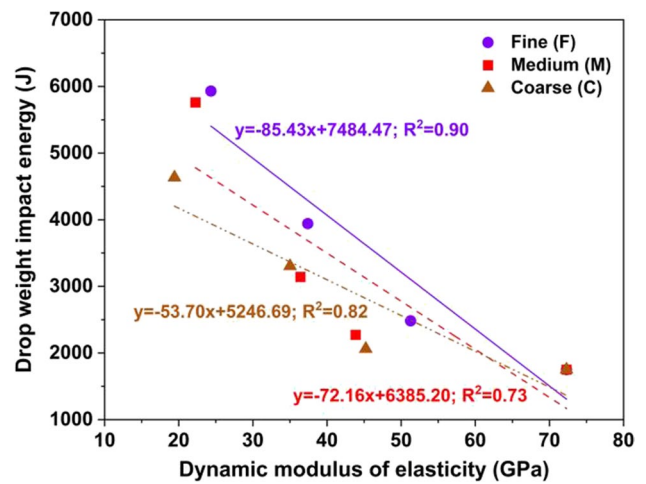


**Fig. 14** Relation between dynamic modulus of elasticity and drop weight impact energy

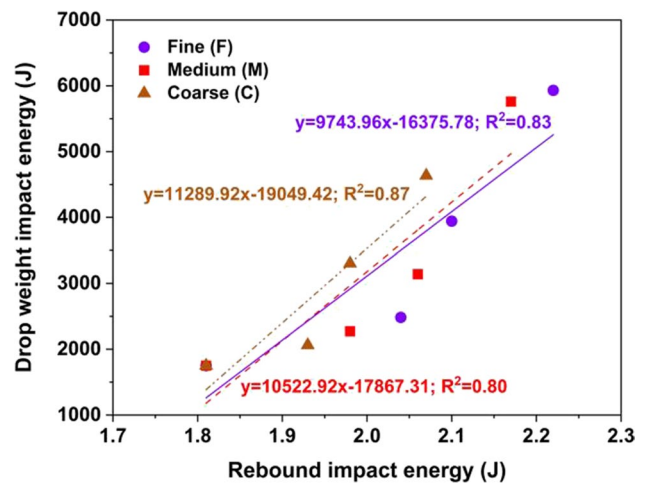


**Fig. 15** Relation between rebound impact energy and drop weight impact energy

mixes by researchers in the past (Gupta et al. 2015a, 2017b; Mastali et al. 2016; Mastali and Dalvand 2016; Moghadam et al. 2021; Rahmani et al. 2012; Xiang-yu et al. 2011). Many research studies (Gupta et al. 2015a, 2017b; Moghadam et al. 2021; Xiang-yu et al. 2011) reported that two-parameter Weibull distribution analysis had provided consistent results for studying repeated load test data. Therefore, in the present study, the two-parameter Weibull distribution was selected as a probabilistic model to analyse the drop weight test results using the graphical method. As shown in Eq. (7), a cumulative distribution function  $F(n)$  is used to represent the Weibull two-parameter distribution function in terms of probability density function (Moghadam et al. 2021).

$$F_{(n)} = 1 - e^{-\left(\frac{\alpha}{u}\right)^\alpha} \tag{7}$$

where  $n$ , impact life of concrete;  $\alpha$ , Weibull parameter;  $u$ , scale parameter.

The possibility of survivorship function is given by Eq. (8) (Moghadam et al. 2021).

$$L_N = 1 - F_{(n)} = e^{-\left(\frac{\alpha}{u}\right)^\alpha} \tag{8}$$

By performing double natural logarithmic operations on both sides of Eq. (8), we gain,

$$\ln\left(\ln\left(\frac{1}{L_N}\right)\right) = \alpha \ln(n) - \alpha \ln(u) \tag{9}$$

The linear relationship in Eq. (9), between  $\ln(\ln(1/L_N))$  and  $\ln(n)$ , is used to authenticate the number of impacts  $N_1$  and  $N_2$ . The physical investigation survivorship function  $L_N$  for the number of impacts  $N_1$  and  $N_2$  is determined from Eq. (10).

$$L_N = 1 - \frac{i}{t + 1} \tag{10}$$

where  $i$ , rank of failed sample and  $t$ , the total number of test samples for a particular series.

The results obtained in the Weibull two-parameter distribution analysis are reliable when the relation between  $\ln(\ln(1/L_N))$  and  $\ln(n)$  is fit for linear regression. The graphical representation of the relationship obtained in the Weibull two-parameter distribution is shown in Fig. 16 for  $N_1$  and in Fig. 17 for  $N_2$ . The regression constants of Eq. (9) ( $\alpha$  and  $\alpha \ln(u)$ ) for  $N_1$  and  $N_2$  (showed in Table 5) were obtained by determining the equation of the straight line of graphical plot between  $\ln(\ln(1/L_N))$  and  $\ln(n)$ . From Table 5, it was observed that the

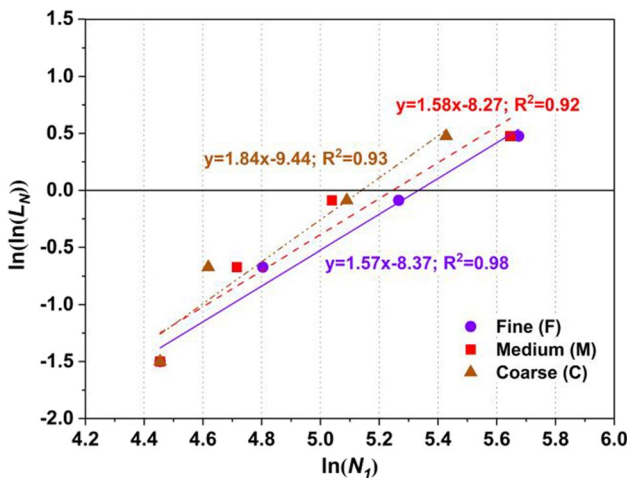


Fig. 16 Weibull distribution for the number of impacts at the first crack ( $N_1$ )

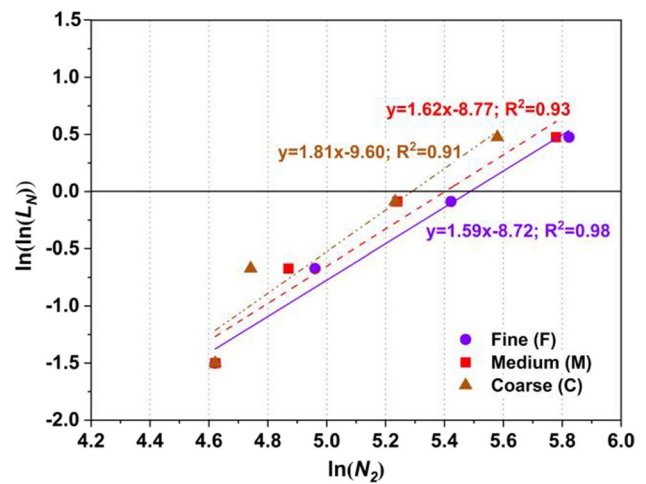


Fig. 17 Weibull distribution for the number of impacts at the ultimate failure ( $N_2$ )

correlation coefficient ( $R^2$ ) for each series (fine, medium, and coarse fibre size) of  $N_1$  and  $N_2$  is greater than 0.90. Therefore, it can be summarised that the Weibull two-parameter distribution is dependable for statistical analysis of drop weight impact energy  $I_{f,dw}$  and  $I_{u,dw}$  of SCC with WTR fibre.

The experimental investigation carried out in this study showed the effect of replacement ratios and size variation of WTR fibre on mobility and stability of fresh SCC, density, compressive strength, static MOE, dynamic MOE, rebound impact resistance, and drop weight impact resistance of hardened SCC. Test results showed that the fibre shape of WTR hindered the mobility; however, it improved the stability in terms of segregation resistance of SCC. In the hardened state, the incorporation of WTR fibre resulted in poor microstructural characteristics and density, which further affected the compressive strength with the increased replacement ratios and particle size of WTR fibre. The induced porous structure, material non-homogeneity, and low stiffness of rubber led to decreased static and dynamic MOE on the incorporation of WTR fibre in SCC. The reduced stiffness of the matrix and increased deformability due to rubber incorporation enhanced the concrete’s energy dissipation

Table 5 Regression constants and correlation coefficient of linear regression analysis in Weibull distribution

Number of impacts	Fibre size	Regression constant ( $\alpha$ )	Regression constant ( $\alpha \ln u$ )	Correlation coefficient ( $R^2$ )
$N_1$	Fine	1.57	8.37	0.98
	Medium	1.58	8.27	0.92
	Coarse	1.84	9.44	0.93
$N_2$	Fine	1.59	8.72	0.98
	Medium	1.62	8.77	0.93
	Coarse	1.81	9.60	0.91



capacity. The increased rebound impact and drop weight impact resistance indicated the effect of enhanced energy dissipation capacity of rubberised SCC. Moreover, the fibre shape and high flexibility of WTR improved the post-failure impact resistance of SCC, which further increased with the increased replacement levels of NFA. The highest impact resistance is observed for fine fibre incorporated SCC mixes, followed by medium and coarse fibre SCC mixes.

Despite the reduction in density and compressive strength of WTR fibre, incorporated SCC can be implemented for environment-friendly construction practices with low strength requirement applications such as cement-based masonry bricks and blocks, partition panels, lightweight blocks, roadside kerbs, precast door frames, drainage channels. The replacement of NFA with WTR fibre can be practised at places where competent authorities ban excavating river beds to conserve the river ecosystem. The use of WTR fibre as fine aggregate in cementitious mixes can be encouraged in countries where the conventional disposal methods (landfilling and stockpiling) of waste tyres are restricted, and waste tyres are exported to other countries like India for waste management (Inton 2019; Karger-Kocsis et al. 2013; Luhar et al. 2018). Along with the environment-friendly practices, i.e., conservation of natural resources and effective waste disposal methods, incorporating WTR fibre as fine aggregate improves the ductility of SCC. Due to a reduction in MOE and around 4.5 times improvement in impact resistance as compared to the control mix, the rubberised SCC can be implemented for high ductility requirement concrete applications. The use of WTR fibre as fine aggregate can be practised for developing paver blocks for light, medium, and heavy traffic loads, impact absorbance flooring tiles, crash barriers, waterfront retaining structures, flooring of goods loading and unloading yards, etc. Moreover, based on the results of size variation of WTR fibre on fresh and hardened properties of SCC, field practitioners can decide the replacement level of NFA for the available onsite size of WTR fibre.

## Conclusions

To examine the static and impact load resistance of self-compacting concrete (SCC) comprising waste tyre rubber (WTR) fibre, three different sizes of 0.60–1.18 mm (fine), 1.18–2.36 mm (medium), and 2.36–4.75 mm (coarse) were used as fine aggregate (up to 30%). The following conclusions are drawn from the study:

1. The segregation resistance of SCC improved with the addition of fine, medium, and coarse sizes of WTR fibre. Due to inter-particle friction and fibre overlapping, the higher content and size of WTR fibre decreased the slump flow of SCC with WTR fibre.
2. The use of WTR fibre as fine aggregate reduced the density of SCC due to the difference in their specific gravity. Moreover, due to WTR fibre's hydrophobicity, it traps air, resulting in empty gaps in the cementitious matrix. This demonstrated the direct effect of decreased compressive strength in SCC with WTR fibre. Fine fibre resulted in the lowest decrease in compressive strength relative to the medium and coarse sizes at each replacement level.
3. The water permeability of SCC was increased on the increased WTR fibre content and size. The increased water permeability indicated the more pore spaces in the concrete on the increased WTR fibre content and size.
4. The static modulus of elasticity dropped due to the WTR fibre incorporation, which decreased the stiffness of the cementitious matrix of SCC with WTR fibre. The addition of low-stiffness material, i.e., WTR fibre, seems to boost the deformability of SCC with WTR fibre.
5. The decrease in dynamic modulus of elasticity indicated a high rate of energy dissipation, which increased further as the size of WTR fibre changed from fine to coarse.
6. The addition of WTR fibre increased the number of impacts required to fracture the specimen, indicating a decrease in brittleness or an increase in energy absorption of SCC with WTR fibre. Similarly, the rebound impact test demonstrated higher energy absorption by SCC with WTR fibre, which was highly associated with the drop weight in the linear regression analysis.

**Acknowledgements** The authors are obliged to the Material Research Centre (MRC), MNIT Jaipur, to avail microstructure analysis facilities. The support received from the Department of Science and Technology, DST, Govt. of India under project grant (DST/INT/UK/P-157/2017) is also acknowledged. One of the authors (AAT) is grateful to the IIT Indore for financial assistance as a teaching assistantship.

**Author contribution** All authors contributed to the study's conception and design. Material preparation, data collection, and analysis were performed by AAT, AS, TG, and SC. The first draft of the manuscript was written by AAT and AS, and all authors commented on previous versions of the manuscript. All authors read and approved the final manuscript.

**Funding** The research leading to these results received funding from the Department of Science and Technology, DST, Govt. of India under Grant Agreement No. DST/INT/UK/P-157/2017.

**Data availability** The datasets used and analysed during the current study are available from the corresponding author on reasonable request.

## Declarations

**Ethics approval and consent to participate** Not applicable.

**Consent for publication** Not applicable.

**Competing interests** The authors declare no competing interests.

## References

- AbdelAleem BH, Ismail MK, Hassan AAA (2018) The combined effect of crumb rubber and synthetic fibers on impact resistance of self-consolidating concrete. *Constr Build Mater* 162:816–829. <https://doi.org/10.1016/j.conbuildmat.2017.12.077>
- Abdelmonem A, El-Feky MS, Nasr ESAR, Kohail M (2019) Performance of high strength concrete containing recycled rubber. *Constr Build Mater* 227:116660. <https://doi.org/10.1016/j.conbuildmat.2019.08.041>
- ACI 544 (1999) Measurement of properties of fiber reinforced concrete. American Concrete Institute 1–12
- Aïssoun BM, Hwang SD, Khayat KH (2016) Influence of aggregate characteristics on workability of superworkable concrete. *Mater Struct* 49:597–609. <https://doi.org/10.1617/s11527-015-0522-9>
- Al-Hadithi AI, Hilal NN (2016) The possibility of enhancing some properties of self-compacting concrete by adding waste plastic fibers. *J Build Eng* 8:20–28. <https://doi.org/10.1016/j.jobbe.2016.06.011>
- Al-Mutairi N, Al-Rukaibi F, Bufarsan A (2010) Effect of microsilica addition on compressive strength of rubberised concrete at elevated temperatures. *J Mater Cycles Waste Manag* 12(1):41–49. <https://doi.org/10.1007/s10163-009-0243-7>
- Aliabdo AA, Abd Elmoaty AEM, Abdelbaset MM (2015) Utilisation of waste rubber in non-structural applications. *Constr Build Mater* 91:195–207. <https://doi.org/10.1016/j.conbuildmat.2015.05.080>
- Angelin AF, Andrade MFFF, Bonatti R, Lintz RCC, Gachet-barbosa LA, Osório WR (2015) Effects of spheroid and fiber-like waste-tire rubbers on interrelation of strength-to-porosity in rubberised cement and mortars. *Constr Build Mater* 95:525–536. <https://doi.org/10.1016/j.conbuildmat.2015.07.166>
- Angelin AF, Cecche Lintz RC, Osório WR, Gachet LA (2020) Evaluation of efficiency factor of a self-compacting lightweight concrete with rubber and expanded clay contents. *Constr Build Mater* 257:119573. <https://doi.org/10.1016/j.conbuildmat.2020.119573>
- Angelin AF, Da Silva FM, Barbosa LAG, Lintz RCC, De Carvalho MAG, Franco RAS (2017) Voids identification in rubberised mortar digital images using k-means and watershed algorithms. *J Clean Prod* 164:455–464. <https://doi.org/10.1016/j.jclepro.2017.06.202>
- Angelin AF, Lintz RCC, Gachet-Barbosa LA, Osório WR (2017) The effects of porosity on mechanical behavior and water absorption of an environmentally friendly cement mortar with recycled rubber. *Constr Build Mater* 151:534–545. <https://doi.org/10.1016/j.conbuildmat.2017.06.061>
- Angelin AF, Miranda EJP, Santos JMCD, Lintz RCC, Gachet-Barbosa LA (2019) Rubberised mortar: the influence of aggregate granulometry in mechanical resistances and acoustic behavior. *Constr Build Mater* 200:248–254. <https://doi.org/10.1016/j.conbuildmat.2018.12.123>
- Arulmoly B, Konthesingha C, Nanayakkara A (2021) Performance evaluation of cement mortar produced with manufactured sand and offshore sand as alternatives for river sand. *Constr Build Mater* 297:123784. <https://doi.org/10.1016/j.conbuildmat.2021.123784>
- As'ad S, Gunawan P, Alaydrus MS (2011) Fresh state behavior of self compacting concrete containing waste material fibres, In: Proceedings of the Twelfth East Asia-Pacific Conference on Structural Engineering and Construction. Elsevier B.V. 797–804. <https://doi.org/10.1016/j.proeng.2011.07.101>
- Aslani F, Gedeon R (2019) Experimental investigation into the properties of self-compacting rubberised concrete incorporating polypropylene and steel fibers. *Struct Concr* 20(1):267–281. <https://doi.org/10.1002/suco.201800182>
- Aslani F, Khan M (2019) Properties of high-performance self-compacting rubberised concrete exposed to high temperatures. *J Mater Civ Eng* 31(5):1–15. [https://doi.org/10.1061/\(ASCE\)MT.1943-5533.0002672](https://doi.org/10.1061/(ASCE)MT.1943-5533.0002672)
- ASTM C 469 (2002) Standard test method for static modulus of elasticity and poisson's ratio of concrete in compression. American Society for Testing and Materials 1–5
- ASTM C 642 (2013) Standard test method for density, absorption, and voids in hardened concrete. American Society for Testing and Materials 1–3
- Ataei H (2016) Experimental study of rubber tire aggregates effect on compressive and dynamic load-bearing properties of cylindrical concrete specimens. *J Mater Cycles Waste Manag* 18(4):665–676. <https://doi.org/10.1007/s10163-015-0362-2>
- Ba Thai Q, Ee Siang T, Le Khac D, Shah WA, Phan-Thien N, Duong HM (2019) “Advanced fabrication and multi-properties of rubber aerogels from car tire waste”, *Colloids Surfaces A Physicochem. Eng Asp* 577:702–708. <https://doi.org/10.1016/j.colsurfa.2019.06.029>
- Bandarage K, Sadeghian P (2020) Effects of long shredded rubber particles recycled from waste tires on mechanical properties of concrete. *J Sustain Cem Mater* 9(1):50–59. <https://doi.org/10.1080/21650373.2019.1676839>
- Bideci A, Öztürk H, Bideci ÖS, Emiroğlu M (2017) Fracture energy and mechanical characteristics of self-compacting concretes including waste bladder tyre. *Constr Build Mater* 149:669–678. <https://doi.org/10.1016/j.conbuildmat.2017.05.191>
- BIS 13311 (1992) Non-destructive testing of concrete - methods of test, part 1 - ultrasonic pulse velocity. Bureau of Indian Standards New Delhi, India, pp 1–7
- BIS 3812 (2013) Specification for pulverised fuel ash, part-1: for use as pozzolana in cement, cement mortar and concrete. Bureau of Indian Standards New Delhi, India, pp 1–12
- BIS 516 (2004) Methods of tests for strength of concrete. Bureau of Indian Standards (Reaffirmed 1999) 1–23
- BIS 8112 (2013) Ordinary portland cement, 43 grade - specification. Bureau of Indian Standards New Delhi India (March)
- Callinan G, Cashman G (2005) Retaining wall system, Patent Pub. No. US 2005/0042039 A1
- Cao M, Xu L, Zhang C (2016) Rheology, fiber distribution and mechanical properties of calcium carbonate (caco3) whisker reinforced cement mortar. *Compos Part A Appl Sci Manuf* 90:662–669. <https://doi.org/10.1016/j.compositesa.2016.08.033>
- Cao M, Xu L, Zhang C (2018) Rheological and mechanical properties of hybrid fiber reinforced cement mortar. *Constr Build Mater* 171:736–742. <https://doi.org/10.1016/j.conbuildmat.2017.09.054>
- Chapman MG, Clynick BG (2006) Experiments testing the use of waste material in estuaries as habitat for subtidal organisms. *J Exp Mar Bio Ecol* 338(2):164–178. <https://doi.org/10.1016/j.jembe.2006.06.018>
- Da Silva FM, Gachet Barbosa LA, Cecche Lintz RC, Jacintho AEPGA (2015) Investigation on the properties of concrete tactile paving blocks made with recycled tire rubber. *Constr Build Mater* 91:71–79. <https://doi.org/10.1016/j.conbuildmat.2015.05.027>
- DIN 1048 Part 5 (1991) Testing concrete: testing of hardened concrete (specimens prepared in mould), German Institute for Standardisation
- EFNARC (2005) The european guidelines for self-compacting concrete: specification, production and use, European Federation for Specialist Construction Chemicals and Concrete 1–63
- Eldin NN, Senouci AB (1993) Rubber-tire particles as concrete aggregate. *J Mater Civ Eng* 5(4):478–496. [https://doi.org/10.1061/\(asce\)0899-1561\(1993\)5:4\(478\)](https://doi.org/10.1061/(asce)0899-1561(1993)5:4(478))
- Fernández-Ruiz MA, Gil-Martín LM, Carbonell-Márquez JF, Hernández-Montes E (2018) Epoxy resin and ground tyre rubber replacement for cement in concrete: compressive behaviour and durability properties. *Constr Build Mater* 173:49–57. <https://doi.org/10.1016/j.conbuildmat.2018.04.004>

- Ganjian E, Khorami M, Maghsoudi AA (2009) Scrap-tyre-rubber replacement for aggregate and filler in concrete. *Constr Build Mater* 23(5):1828–1836. <https://doi.org/10.1016/j.conbuildmat.2008.09.020>
- Gesoğlu M, Güneyisi E, Khoshnaw G, İpek S (2014) Investigating properties of pervious concrete containing waste tire rubbers. *Constr Build Mater* 63:206–213. <https://doi.org/10.1016/j.conbuildmat.2014.04.046>
- Ghasemzadeh Z, Sadeghieh A, Shishebori D (2021) A stochastic multi-objective closed-loop global supply chain concerning waste management: a case study of the tire industry. *Environ Dev Sustain* 23(4):5794–5821. <https://doi.org/10.1007/s10668-020-00847-2>
- Girskas G, Nagrockienė D (2017) Crushed rubber waste impact of concrete basic properties. *Constr Build Mater* 140:36–42. <https://doi.org/10.1016/j.conbuildmat.2017.02.107>
- Güneyisi E, Gesoğlu M, Naji N, İpek S (2016) Evaluation of the rheological behavior of fresh self-compacting rubberised concrete by using the herschel-bulkley and modified bingham models. *Arch Civ Mech Eng* 16(1):9–19. <https://doi.org/10.1016/j.acme.2015.09.003>
- Güneyisi E, Gesoğlu M, Özturan T (2004) Properties of rubberised concretes containing silica fume. *Cem Concr Res* 34(12):2309–2317. <https://doi.org/10.1016/j.cemconres.2004.04.005>
- Gupta H, Bansal PP, Sharma R (2021) Development of high-performance hybrid fiber reinforced concrete using different fine aggregates. *Adv Concr Constr* 11(1):19–32. <https://doi.org/10.12989/acc.2021.11.1.019>
- Gupta T, Chaudhary S, Sharma RK (2014) Assessment of mechanical and durability properties of concrete containing waste rubber tire as fine aggregate. *Constr Build Mater* 73:562–574. <https://doi.org/10.1016/j.conbuildmat.2014.09.102>
- Gupta T, Chaudhary S, Sharma RK (2016) Mechanical and durability properties of waste rubber fiber concrete with and without silica fume. *J Clean Prod* 112:702–711. <https://doi.org/10.1016/j.jclepro.2015.07.081>
- Gupta T, Sharma RK, Chaudhary S (2015) Impact resistance of concrete containing waste rubber fiber and silica fume. *Int J Impact Eng* 83:76–87. <https://doi.org/10.1016/j.ijimpeng.2015.05.002>
- Gupta T, Sharma RK, Chaudhary S (2015) Influence of waste tyre fibers on strength, abrasion resistance and carbonation of concrete. *Sci Iran Trans A Civ Eng* 22(4):1481–1489. [http://scien.tiainica.sharif.edu/article\\_1970\\_7b7833b5ac4676974f03e68b16cb76df.pdf](http://scien.tiainica.sharif.edu/article_1970_7b7833b5ac4676974f03e68b16cb76df.pdf)
- Gupta T, Siddique S, Sharma RK, Chaudhary S (2017) Effect of elevated temperature and cooling regimes on mechanical and durability properties of concrete containing waste rubber fiber. *Constr Build Mater* 137:35–45. <https://doi.org/10.1016/j.conbuildmat.2017.01.065>
- Gupta T, Siddique S, Sharma RK, Chaudhary S (2019) Behaviour of waste rubber powder and hybrid rubber concrete in aggressive environment. *Constr Build Mater* 217:283–291. <https://doi.org/10.1016/j.conbuildmat.2019.05.080>
- Gupta T, Siddique S, Sharma RK, Chaudhary S (2021) Investigating mechanical properties and durability of concrete containing recycled rubber ash and fibers. *J Mater Cycles Waste Manag* 23(3):1048–1057. <https://doi.org/10.1007/s10163-021-01192-w>
- Gupta T, Tiwari A, Siddique S, Sharma RK, Chaudhary S (2017) Response assessment under dynamic loading and microstructural investigations of rubberised concrete. *J Mater Civ Eng* 29(8):4017062. [https://doi.org/10.1061/\(ASCE\)MT.1943-5533.0001905](https://doi.org/10.1061/(ASCE)MT.1943-5533.0001905)
- Hernández-Olivares F, Barluenga G (2004) Fire performance of recycled rubber-filled high-strength concrete. *Cem Concr Res* 34(1):109–117
- Hernández-Olivares F, Barluenga G, Parga-Landa B, Bollati M, Witoszek B (2007) Fatigue behaviour of recycled tyre rubber-filled concrete and its implications in the design of rigid pavements. *Constr Build Mater* 21(10):1918–1927. <https://doi.org/10.1016/j.conbuildmat.2006.06.030>
- Herrero S, Mayor P, Hernández-Olivares F (2013) Influence of proportion and particle size gradation of rubber from end-of-life tires on mechanical, thermal and acoustic properties of plaster-rubber mortars. *Mater Des* 47:633–642. <https://doi.org/10.1016/j.matdes.2012.12.063>
- Hesami S, Salehi Hikouei I, Emadi SAA (2016) Mechanical behavior of self-compacting concrete pavements incorporating recycled tire rubber crumb and reinforced with polypropylene fiber. *J Clean Prod* 133:228–234. <https://doi.org/10.1016/j.jclepro.2016.04.079>
- Hilal NN (2017) Hardened properties of self-compacting concrete with different crumb rubber size and content. *Int J Sustain Built Environ* 6(1):191–206. <https://doi.org/10.1016/j.ijsbe.2017.03.001>
- Inton C (2019) The true cost of toxic tyres, URL <https://graphics.reuters.com/ASIA-WASTE-TYRES/0100B2H31RW/index.html>. Accessed 16 Apr 2021
- Ismail MK, Hassan AAA (2017) Impact resistance and mechanical properties of self-consolidating rubberised concrete reinforced with steel fibers. *J Mater Civ Eng* 29(1). [https://doi.org/10.1061/\(ASCE\)MT.1943-5533.0001731](https://doi.org/10.1061/(ASCE)MT.1943-5533.0001731)
- Jain A, Gupta R, Chaudhary S (2020) Sustainable development of self-compacting concrete by using granite waste and fly ash. *Constr Build Mater* 262:120516. <https://doi.org/10.1016/j.conbuildmat.2020.120516>
- Jain D, Sharma R, Bansal PP (2021) Potential use of sillimanite sand in sustainable geopolymer concrete production. *J Mater Civ Eng* 33(8):1–17. [https://doi.org/10.1061/\(asce\)mt.1943-5533.0003826](https://doi.org/10.1061/(asce)mt.1943-5533.0003826)
- Kaewunruen S, Meesit R, Mondal P (2017) Early-age dynamic moduli of crumbed rubber concrete for compliant railway structures. *J Sustain Cem Mater* 6(5):281–292. <https://doi.org/10.1080/21650373.2017.1280425>
- Karakurt C (2015) Microstructure properties of waste tire rubber composites: an overview. *J Mater Cycles Waste Manag* 17(3):422–433. <https://doi.org/10.1007/s10163-014-0263-9>
- Karger-Kocsis J, Mészáros L, Bárány T (2013) Ground tyre rubber (gtr) in thermoplastics, thermosets, and rubbers. *J Mater Sci* 48(1):1–38. <https://doi.org/10.1007/s10853-012-6564-2>
- Karimi A, Nematzadeh M, Mohammad-Ebrahimzadeh-Sepasgozar S (2020) Analytical post-heating behavior of concrete-filled steel tubular columns containing tire rubber. *Comput Concr* 26(12):467–482. <https://doi.org/10.12989/cac.2020.26.6.467>
- Khalil E, Abd-Elmohsen M, Anwar AM (2015) Impact resistance of rubberised self-compacting concrete. *Water Sci* 29(1):45–53. <https://doi.org/10.1016/j.wsj.2014.12.002>
- Khaloo AR, Dehestani M, Rahmatbadi P (2008) Mechanical properties of concrete containing a high volume of tire-rubber particles. *Waste Manag* 28(12):2472–2482. <https://doi.org/10.1016/j.wasman.2008.01.015>
- Li G, Garrick G, Eggers J, Abadie C, Stubblefield MA, Pang SS (2004) Waste tire fiber modified concrete. *Compos Part B Eng* 35(4):305–312. <https://doi.org/10.1016/j.compositesb.2004.01.002>
- Li G, Stubblefield MA, Garrick G, Eggers J, Abadie C, Huang B (2004) Development of waste tire modified concrete. *Cem Concr Res* 34(12):2283–2289. <https://doi.org/10.1016/j.cemconres.2004.04.013>
- Li N, Long G, Ma C, Fu Q, Zeng X, Ma K, Xie Y, Luo B (2019) Properties of self-compacting concrete (scc) with recycled tire rubber aggregate: a comprehensive study. *J Clean Prod* 236:117707. <https://doi.org/10.1016/j.jclepro.2019.117707>
- Long G, Feys D, Khayat KH, Yahia A (2014) Efficiency of waste tire rubber aggregate on the rheological properties and compressive strength of cementitious materials. *J Sustain Cem Mater* 3(3–4):201–211. <https://doi.org/10.1080/21650373.2014.898597>
- Luhar S, Chaudhary S, Luhar I (2018) Thermal resistance of fly ash based rubberised geopolymer concrete. *J Build Eng* 19:420–4328. <https://doi.org/10.1016/j.jobbe.2018.05.025>

- Luhar S, Chaudhary S, Luhar I (2019) Development of rubberised geopolymer concrete: strength and durability studies. *Constr Build Mater* 204:740–753. <https://doi.org/10.1016/j.conbuildmat.2019.01.185>
- Maho B, Sukontasukkul P, Jamnam S, Yamaguchi E, Fujikake K, Bantia N (2019) Effect of rubber insertion on impact behavior of multilayer steel fiber reinforced concrete bulletproof panel. *Constr Build Mater* 216:476–484. <https://doi.org/10.1016/j.conbuildmat.2019.04.243>
- Marie I (2016) Zones of weakness of rubberised concrete behavior using the UPV. *J Clean Prod* 116:217–222. <https://doi.org/10.1016/j.jclepro.2015.12.096>
- Mastali M, Dalvand A (2016) The impact resistance and mechanical properties of self-compacting concrete reinforced with recycled crfp pieces. *Compos Part B Eng* 92:360–376. <https://doi.org/10.1016/j.compositesb.2016.01.046>
- Mastali M, Dalvand A, Sattarifard AR (2016) The impact resistance and mechanical properties of reinforced self-compacting concrete with recycled glass fibre reinforced polymers. *J Clean Prod* 124:312–324. <https://doi.org/10.1016/j.jclepro.2016.02.148>
- Mhaya AM, Fahim Huseien G, Faridmehr I, Razin Zainal Abidin A, Alyousef R, Ismail M (2021) Evaluating mechanical properties and impact resistance of modified concrete containing ground blast furnace slag and discarded rubber tire crumbs. *Constr Build Mater* 295:123603. <https://doi.org/10.1016/j.conbuildmat.2021.123603>
- Mistry MK, Shukla SJ, Solanki CH (2021) Reuse of waste tyre products as a soil reinforcing material: a critical review. *Environ Sci Pollut Res* 28(20):24940–24971. <https://doi.org/10.1007/s11356-021-13522-4>
- Moghadam AS, Omidinasab F, Moazami Goodarzi S (2021) Characterisation of concrete containing RCA and GGBFS: mechanical, microstructural and environmental properties. *Constr Build Mater* 289:123134. <https://doi.org/10.1016/j.conbuildmat.2021.123134>
- Mohajerani A, Burnett L, Smith JV, Markovski S, Rodwell G, Rahman MT, Kurmus H, Mirzababaei M, Arulrajah A, Horpibulsuk S, Maghool F (2020) “Recycling waste rubber tyres in construction materials and associated environmental considerations: a review.” *Resour Conserv Recycl* 155:104679. <https://doi.org/10.1016/j.resconrec.2020.104679>
- Na O, Xi Y (2017) Mechanical and durability properties of insulation mortar with rubber powder from waste tires. *J Mater Cycles Waste Manag* 19(2):763–773. <https://doi.org/10.1007/s10163-016-0475-2>
- Najim KB, Hall MR (2010) A review of the fresh/hardened properties and applications for plain- (prc) and self-compacting rubberised concrete (scrc). *Constr Build Mater* 24(11):2043–2051. <https://doi.org/10.1016/j.conbuildmat.2010.04.056>
- Nematzadeh M, Hosseini SA, Ozbakkaloglu T (2021) The combined effect of crumb rubber aggregates and steel fibers on shear behavior of gfrp bar-reinforced high-strength concrete beams. *J Build Eng* 44:102981. <https://doi.org/10.1016/j.job.2021.102981>
- Nematzadeh M, Mousavi R (2021) Post-fire flexural behavior of functionally graded fiber-reinforced concrete containing rubber. *Comput Concr* 27(5):417–435. <https://doi.org/10.12989/cac.2021.27.5.417>
- Pacheco-Torgal F, Ding Y, Jalali S (2012) Properties and durability of concrete containing polymeric wastes (tyre rubber and polyethylene terephthalate bottles): an overview. *Constr Build Mater* 30:714–724. <https://doi.org/10.1016/j.conbuildmat.2011.11.047>
- Pham TM, Elchalakani M, Karrech A, Hao H (2018) Axial impact behavior and energy absorption of rubberised concrete with/without fiber-reinforced polymer confinement. *Int J Prot Struct* 10(2). <https://doi.org/10.1177/2041419618800771>
- Raghavan D, Huynh H, Ferraris CF (1998) Workability, mechanical properties, and chemical stability of a recycled tyre rubber-filled cementitious composite. *J Mater Sci* 33(7):1745–1752. <https://doi.org/10.1023/A:1004372414475>
- Rahat Dahmardeh S, Sargazi Moghaddam MS, Mirabi Moghaddam MH (2019) Effects of waste glass and rubber on the scc: rheological, mechanical, and durability properties *Eur J Environ Civ Eng* 0(0), 1–20. <https://doi.org/10.1080/19648189.2018.1528891>
- Rahman MM, Usman M, Al-Ghalib AA (2012) Fundamental properties of rubber modified self-compacting concrete (RMSCC). *Constr Build Mater* 36:630–637. <https://doi.org/10.1016/j.conbuildmat.2012.04.116>
- Rahmani T, Kiani B, Shekarchi M, Safari A (2012) Statistical and experimental analysis on the behavior of fiber reinforced concretes subjected to drop weight test. *Constr Build Mater* 37:360–369. <https://doi.org/10.1016/j.conbuildmat.2012.07.068>
- Recycling magazine (2020) URL <https://www.recycling-magazine.com/2020/10/20/nextlap-seeks-for-innovation-for-end-of-life-tire-market/>. Accessed 15 Apr 2021
- Reda Taha MM, El-Deib AS, El-wahab MAA, Abdel-Hameed ME (2008) Mechanical, fracture, and microstructural investigations of rubber concrete. *J Mater Civ Eng* 20(10):640–649. [https://doi.org/10.1061/\(ASCE\)0899-1561\(2008\)20:10\(640\)](https://doi.org/10.1061/(ASCE)0899-1561(2008)20:10(640))
- Sabetifar H, Nematzadeh M, Gholampour A (2022) Modeling of heated concrete-filled steel tubes with steel fiber and tire rubber under axial compression. *Comput Concr* 29(1):15–29. <https://doi.org/10.12989/cac.2022.29.1.015>
- Shen W, Shan L, Zhang T, Ma H, Cai Z, Shi H (2013) Investigation on polymer-rubber aggregate modified porous concrete. *Constr Build Mater* 38:667–674. <https://doi.org/10.1016/j.conbuildmat.2012.09.006>
- Shu X, Huang B (2014) Recycling of waste tire rubber in asphalt and portland cement concrete: an overview. *Constr Build Mater* 67:217–224. <https://doi.org/10.1016/j.conbuildmat.2013.11.027>
- Sibeko MA, Adeniji AO, Okoh OO, Hlangothi SP (2020) Trends in the management of waste tyres and recent experimental approaches in the analysis of polycyclic aromatic hydrocarbons (pahs) from rubber crumbs. *Environ Sci Pollut Res* 27(35):43553–43568. <https://doi.org/10.1007/s11356-020-09703-2>
- Siddique S, Gupta T, Thakare AA, Gupta V, Chaudhary S (2019) Acid resistance of fine bone China ceramic aggregate concrete. *Eur J Environ Civ Eng* 25(7):1219–1232. <https://doi.org/10.1080/19648189.2019.1572543>
- Su H, Yang J, Ling TC, Ghataora GS, Dirar S (2015) Properties of concrete prepared with waste tyre rubber particles of uniform and varying sizes. *J Clean Prod* 91:288–296. <https://doi.org/10.1016/j.jclepro.2014.12.022>
- Thakare AA, Siddique S, Sarode SN, Deewan R, Gupta V, Gupta S, Chaudhary S (2020a) A study on rheological properties of rubber fiber dosed self-compacting mortar. *Constr Build Mater* 262:120745. <https://doi.org/10.1016/j.conbuildmat.2020.120745>
- Thakare AA, Singh, A, Gupta V, Siddique S, Chaudhary S (2020b) Sustainable development of self-compacting cementitious mixes using waste originated fibers: a review. *Resour Conserv Recycl* 168. <https://doi.org/10.1016/j.resconrec.2020b.105250>
- Thakare AA, Gupta T, Deewan R, Chaudhary S (2022a) Micro and macro-structural properties of waste tyre rubber fibre-reinforced bacterial self-healing mortar *Constr Build Mater* 322. <https://doi.org/10.1016/j.conbuildmat.2022.126459>
- Thakare AA, Siddique S, Singh A, Gupta T, Chaudhary S (2022b) Effect of rubber fiber size fraction on static and impact behaviour of self compacting concrete. *Adv Concr Constr* 13(6):433–450. <https://doi.org/10.12989/acc.2022.13.6.433>
- Thomas BS, Gupta RC (2016) A comprehensive review on the applications of waste tire rubber in cement concrete. *Renew Sustain Energy Rev* 54:1323–1333. <https://doi.org/10.1016/j.rser.2015.10.092>

- Topçu İB, Demir A (2007) Durability of rubberised mortar and concrete. *J Mater Civ Eng* 19:173–178. [https://doi.org/10.1061/\(ASCE\)0899-1561\(2007\)19:2\(173\)](https://doi.org/10.1061/(ASCE)0899-1561(2007)19:2(173))
- Tsang HH, Sheikh MN, Lam N (2007) Rubber-soil cushion for earthquake protection. In: Lam N, Wilson J, Gibson G, Anderson S (eds) Australian Earthquake Engineering Society Conference. Australian Earthquake Engineering Society, Australia, pp 1–8
- Turatsinze A, Garros M (2008) On the modulus of elasticity and strain capacity of self-compacting concrete incorporating rubber aggregates. *Resour Conserv Recycl* 52(10):1209–1215. <https://doi.org/10.1016/j.resconrec.2008.06.012>
- Uygunoğlu T, Topçu İB (2010) The role of scrap rubber particles on the drying shrinkage and mechanical properties of self-consolidating mortars. *Constr Build Mater* 24(7):1141–1150. <https://doi.org/10.1016/j.conbuildmat.2009.12.027>
- WBCSD and The Tire Industry Project (2019) Global elt management—a global state of knowledge on regulation, management systems, impacts of recovery and technologies (December). [https://docs.wbcsd.org/2019/12/Global\\_ELT\\_Management%E2%80%933A\\_global\\_state\\_of\\_knowledge\\_on\\_regulation\\_management\\_systems\\_impacts\\_of\\_recovery\\_and\\_technologies.pdf](https://docs.wbcsd.org/2019/12/Global_ELT_Management%E2%80%933A_global_state_of_knowledge_on_regulation_management_systems_impacts_of_recovery_and_technologies.pdf)
- Xiang-yu C, Yi-ning D, Azevedo C (2011) Combined effect of steel fibres and steel rebars on impact resistance of high performance concrete. *J Cent South Univ Technol* 18:1677–1684. <https://doi.org/10.1007/s11771>
- Xu W, Wen X, Wei J, Xu P, Zhang B, Yu Q, Ma H (2018) Feasibility of kaolin tailing sand to be as an environmentally friendly alternative to river sand in construction applications. *J Clean Prod* 205:1114–1126. <https://doi.org/10.1016/j.jclepro.2018.09.119>
- Yaragal SC, Basavana Gowda SN, Rajasekaran C (2019) Characterisation and performance of processed lateritic fine aggregates in cement mortars and concretes. *Constr Build Mater* 200:10–25. <https://doi.org/10.1016/j.conbuildmat.2018.12.072>
- Yeo JS, Koting S, Onn CC, Mo KH (2021) An overview on the properties of eco-friendly concrete paving blocks incorporating selected waste materials as aggregate. *Environ Sci Pollut Res* 28(23):29009–29036. <https://doi.org/10.1007/s11356-021-13836-3>
- Yilmaz A, Degirmenci N (2009) Possibility of using waste tire rubber and fly ash with portland cement as construction materials. *Waste Manag* 29(5):1541–1546. <https://doi.org/10.1016/j.wasman.2008.11.002>
- Youssif O, Hassanli R, Mills JE (2017) Mechanical performance of frp-confined and unconfined crumb rubber concrete containing high rubber content. *J Build Eng* 11:115–126. <https://doi.org/10.1016/j.jobe.2017.04.011>
- Zaharia M, Sahajwalla V, Kim BC, Khanna R, Saha-Chaudhury N, O’Kane P, Dicker J, Skidmore C, Knights D (2009) Recycling of rubber tires in electric arc furnace steelmaking: simultaneous combustion of metallurgical coke and rubber tyres blends. *Energy Fuels* 23(5):2467–2474. <https://doi.org/10.1021/ef8010788>
- Zamanzadeh Z, Lourenço L, Barros J (2015) Recycled steel fibre reinforced concrete failing in bending and in shear. *Constr Build Mater* 85:195–207. <https://doi.org/10.1016/j.conbuildmat.2015.03.070>

**Publisher's Note** Springer Nature remains neutral with regard to jurisdictional claims in published maps and institutional affiliations.

Springer Nature or its licensor holds exclusive rights to this article under a publishing agreement with the author(s) or other rightsholder(s); author self-archiving of the accepted manuscript version of this article is solely governed by the terms of such publishing agreement and applicable law.